

Distillation of RL Policies with Formal Guarantees via Variational Abstraction of Markov Decision Processes

Technical Report

Florent Delgrange,¹ Ann Nowé,¹ Guillermo A. Pérez²

¹ AI Lab, Vrije Universiteit Brussel
florent.delgrange@ai.vub.ac.be

² University of Antwerp – Flanders Make

Abstract

We consider the challenge of policy simplification and verification in the context of policies learned through reinforcement learning (RL) in continuous environments. In well-behaved settings, RL algorithms have convergence guarantees in the limit. While these guarantees are valuable, they are insufficient for safety-critical applications. Furthermore, they are lost when applying advanced techniques such as deep-RL. To recover guarantees when applying advanced RL algorithms to more complex environments with (i) reachability, (ii) safety-constrained reachability, or (iii) discounted-reward objectives, we build upon the DeepMDP framework introduced by Gelada et al. to derive new bisimulation bounds between the unknown environment and a learned discrete latent model of it. Our bisimulation bounds enable the application of formal methods for Markov decision processes. Finally, we show how one can use a policy obtained via state-of-the-art RL to efficiently train a variational autoencoder that yields a discrete latent model with provably approximately correct bisimulation guarantees. Additionally, we obtain a distilled version of the policy for the latent model.

1 Introduction

While *reinforcement learning* (RL) has been applied to a wide range of challenging domains, from game playing (Mnih et al. 2015) to real-world applications such as effective canal control (Ren et al. 2021), more widespread deployment in the real world is hampered by the lack of guarantees provided with the learned policies. Although there are RL algorithms which have limit-convergence guarantees in the discrete setting (Tsitsiklis 1994) — and even in some continuous settings with function approximation, e.g., Nowé (1994) — these are lost when applying more advanced techniques which make use of general nonlinear function approximators (Tsitsiklis and Roy 1997) to deal with continuous *Markov decision processes* (MDPs) such as *deep-RL* (e.g., Mnih et al. 2015). In this paper, we apply such advanced RL algorithms to unknown continuous MDPs with (i) reachability, (ii) safety-constrained reachability, or (iii) discounted-reward objectives. To recover the formal guarantees, we use the obtained policy to train a *variational autoencoder* (VAE) which gives us a *discrete latent model* that approximates the unknown environment. We build upon the *DeepMDP* framework (Gelada et al. 2019) to provide guarantees on the quality of the abstraction induced by this

model. DeepMDPs are provided with such guarantees when their *loss functions* are minimized. These can be defined on the entire state space (*global*) or on states visited under a given policy (*local*). The guarantees concern a *state embedding function*, linking the latent and original MDPs and are defined as bounds on the difference of their *value function* and *bisimulation distance*. The latter was only developed for global losses. While these are interesting in theory, they are often infeasible to measure in practice. In contrast, we introduce such bounds in the local setting and further consider an *action embedding function* to handle continuous actions. Importantly, we focus on general MDPs and do not restrict our attention to deterministic ones as was done by Gelada et al. to enable the approximation and minimization of their losses via neural networks. We also give PAC approximation schemes to compute both the losses and said bounds.

Our VAE is trained by maximizing a lower bound on the likelihood of traces generated by executing the RL policy in the environment. We derive a loss function, incorporating variational versions of the local losses, that enables learning (i) discrete state and action spaces, (ii) an MDP defined over these spaces, (iii) state and action embedding functions, linking the original and discrete MDPs, and (iv) a *distilled* version of the RL policy set over the discrete spaces which can be executed in both models via the embedding functions. An important challenge for our approach is the *posterior collapse problem* which often occurs when optimizing a variational model (e.g., Alemi et al. 2018). We present a novel approach based on *prioritized experience replay* (Schaul et al. 2016) to resolve this when learning a discrete latent model.

All of the above result in an efficient way of training a VAE to obtain a discrete latent model that is provably approximately bisimilar to the unknown MDP, further yielding a distilled version of the RL policy. These enable the application of formal methods and tools that have been developed for discrete MDPs: for instance, PRISM (Kwiatkowska, Norman, and Parker 2011), MODEST (Hartmanns and Hermanns 2014), and STORM (Hensel et al. 2021).

Other related work. Frameworks providing formal guarantees *during the RL process* include the work of Junges et al. (2016), *Shielded-RL* (Alshiekh et al. 2018; Jansen et al. 2020), and *AlwaysSafe* (Simão, Jansen, and Spaan 2021). These all require an abstract model of the safety aspect of the environment. Our approach is complementary in that we

assume no prior knowledge and *learn an abstraction*. Notably, our goal is not the same: they aim at verifying whether the exploration is safe while our goal is to verify policies learned via *any* RL technique. Other approaches share ours in the particular case of verifying deep-RL policies, but rely on a known (abstraction of the) environment model. Bacci and Parker (2020) require the neural network (NN) specifying the policy, the environment to be deterministic, and a formal description of the probability of action failures. Carr, Jansen, and Topcu (2020) require the environment to be discrete and focus on policies represented as recurrent NNs by discretizing their hidden states via *quantized* autoencoders, in the same spirit as our policy distillation. Finally, Alamdari et al. (2020) focus on tree-based policies distilled from deep-RL, without considering abstraction quality guarantees.

VAEs have been used in the context of (model-based) RL to learn latent representations of the unknown environment and train simpler policies from the features extracted (e.g., Corneil, Gerstner, and Brea 2018; Freeman, Ha, and Metz 2019; Lee et al. 2020; Burden, Siahroudi, and Kudenko 2021). In particular, Corneil, Gerstner, and Brea (2018) focused on learning discrete latent MDPs from continuous-state environments with discrete actions (without guarantees nor distilled policies) to plan via *prioritized sweeping*.

2 Background

We write $[T] = \{n \in \mathbb{N} \mid n \leq T\}$. For $A \subseteq X$, we denote by $\mathbf{1}_A: X \rightarrow [1]$ the indicator function: $\mathbf{1}_A(a) = 1$ iff $a \in A$. Let \mathcal{X} be a complete and separable space and $\Sigma(\mathcal{X})$ denote the set of all Borel subsets of \mathcal{X} . We write $\mathcal{P}(\mathcal{X})$ for the set of measures P defined on \mathcal{X} and $\text{Supp}(P) = \{x \in \mathcal{X} \mid P(x) > 0\}$ to denote their support.

Discrepancy measures. Let $P, Q \in \mathcal{P}(\mathcal{X})$ with density functions p and q . Their discrepancy can be measured via

- *Kullback-Leibler* (KL) divergence: $D_{\text{KL}}(P \parallel Q) = \mathbb{E}_{x \sim P}[\log(p(x)/q(x))]$.
- *Wasserstein*: $W_d(P, Q) = \inf_{\lambda \in \Lambda(P, Q)} \mathbb{E}_{x, y \sim \lambda} d(x, y)$, where $d: \mathcal{X} \times \mathcal{X} \rightarrow [0, \infty[$ is a distance metric over \mathcal{X} and $\Lambda(P, Q)$ is the set of all *couplings* of P and Q .
- *Total Variation* (TV): $d_{\text{TV}}(P, Q) = \sup_{A \in \Sigma(\mathcal{X})} |P(A) - Q(A)|$. If \mathcal{X} is equipped with the discrete metric $\mathbf{1}_{\neq}$, TV coincides with the Wasserstein measure.

Markov decision processes. A *Markov decision process* (MDP) is a tuple $\mathcal{M} = \langle \mathcal{S}, \mathcal{A}, \mathbf{P}, \mathcal{R}, \ell, \mathbf{AP}, s_I \rangle$ where \mathcal{S} is a set of *states*; \mathcal{A} , a set of *actions*; $\mathbf{P}: \mathcal{S} \times \mathcal{A} \rightarrow \mathcal{P}(\mathcal{S})$, a *probability transition function*; $\mathcal{R}: \mathcal{S} \times \mathcal{A} \rightarrow \mathbb{R}$, a *reward function*; $\ell: \mathcal{S} \rightarrow 2^{\mathbf{AP}}$, a *labeling function* over a set of atomic propositions \mathbf{AP} ; and $s_I \in \mathcal{S}$, the *initial state*. The set of *enabled actions* of $s \in \mathcal{S}$ is $\text{Act}(s) \subseteq \mathcal{A}$. We assume $\text{Act}(s) \neq \emptyset$ for all $s \in \mathcal{S}$. If $|\text{Act}(s)| = 1$ for all $s \in \mathcal{S}$, \mathcal{M} is a fully stochastic process called a *Markov chain* (MC).

Let $\mathbb{T} \subseteq \mathbf{AP}$, we write $\llbracket \mathbb{T} \rrbracket = \{s \mid \ell(s) \cap \mathbb{T} \neq \emptyset\} \subseteq \mathcal{S}$ and $\llbracket \neg \mathbb{T} \rrbracket = \mathcal{S} \setminus \llbracket \mathbb{T} \rrbracket$. We assume \mathbf{AP} and labels being respectively *one-hot* and binary encoded. We write \mathcal{M}_s for the MDP obtained when we replace the initial state of \mathcal{M} by $s \in \mathcal{S}$, $\mathcal{M} \oplus \mathcal{R}'$ when we replace the reward function by \mathcal{R}' , and \mathcal{M}^{OB} when we make absorbing states from

$B \subseteq \mathcal{S}$, i.e., by changing $\mathbf{P}(\cdot \mid s, a)$ to $\mathbf{P}'(\cdot \mid s, a)$ such that $\mathbf{P}'(B \mid s, a) = 1$ for all $s \in B$, $a \in \text{Act}(s)$. We refer to MDPs with continuous states or actions spaces as *continuous MDPs*. In that case, we assume \mathcal{S} and \mathcal{A} are complete separable metric spaces equipped with a Borel σ -algebra and $\ell^{-1}(\mathbb{T}) \in \Sigma(\mathcal{S})$ for any $\mathbb{T} \subseteq \mathbf{AP}$.

Trajectories. A *trajectory* τ of \mathcal{M} is a sequence of states and actions $\tau = \langle s_{0:T}, a_{0:T-1} \rangle$ where $s_0 = s_I$, $s_{t+1} \sim \mathbf{P}(\cdot \mid s_t, a_t)$ and $a_t \in \text{Act}(s_t)$ for $t \in [T-1]$. The set of infinite trajectories of \mathcal{M} is $\text{Traj}_{\mathcal{M}}$. An *execution trace* $\hat{\tau}$ of \mathcal{M} is a trajectory that additionally records labels and rewards encountered. The set of execution traces of \mathcal{M} is $\text{Traces}_{\mathcal{M}}$.

Policies. A (*memoryless*) *policy* $\pi: \mathcal{S} \rightarrow \mathcal{P}(\mathcal{A})$ of \mathcal{M} is a stochastic mapping from states to actions such that $\text{Supp}(\pi(\cdot \mid s)) \subseteq \text{Act}(s)$. The set of memoryless policies of \mathcal{M} is $\Pi_{\mathcal{M}}^{\text{ml}}$. An MDP \mathcal{M} and $\pi \in \Pi_{\mathcal{M}}^{\text{ml}}$ induce an MC \mathcal{M}_{π} along with a unique probability measure $\mathbb{P}_{\pi}^{\mathcal{M}}$ on the Borel σ -algebra over measurable subsets $E \subseteq \text{Traj}_{\mathcal{M}}$ (Puterman 1994). We drop the superscript when the context is clear. For $\pi \in \Pi_{\mathcal{M}}^{\text{ml}}$, we denote by $\mathbf{P}_{\pi}: \mathcal{S} \rightarrow \mathcal{P}(\mathcal{S})$ the probability transition distribution of \mathcal{M}_{π} , and by $\mathcal{R}_{\pi}: \mathcal{S} \rightarrow \mathbb{R}$ its reward function. We write $\hat{\tau} = \langle s_{0:T}, a_{0:T-1}, r_{0:T-1}, l_{0:T} \rangle \sim \mathcal{M}_{\pi}$ for $\langle s_{0:T}, a_{0:T-1} \rangle \sim \mathbb{P}_{\pi}^{\mathcal{M}}$ with $\hat{\tau} \in \text{Traces}_{\mathcal{M}_{\pi}}$.

Stationary distributions. Let $\pi \in \Pi_{\mathcal{M}}^{\text{ml}}$, $\xi_{\pi}^t: \mathcal{S} \rightarrow \mathcal{P}(\mathcal{S})$ with $\xi_{\pi}^t(s' \mid s) = \mathbb{P}_{\pi}^{\mathcal{M}_s}(\{s_{0:\infty}, a_{0:\infty} \mid s_t = s'\})$ be the distribution giving the probability for the agent of being in each state of \mathcal{M}_s after t steps, and $B \subseteq \mathcal{S}$. B is a *strongly connected component* (SCC) of \mathcal{M}_{π} if for any pair of states $s, s' \in B$, $\xi_{\pi}^t(s' \mid s) > 0$ for some $t \in \mathbb{N}$. It is a *bottom SCC* (BSCC) if (i) B is a maximal SCC, and (ii) for each $s \in B$, $\mathbf{P}_{\pi}(B \mid s) = 1$. The unique stationary distribution of B is $\xi_{\pi} \in \mathcal{P}(B)$. We write $s, a \sim \xi_{\pi}$ as shorthand for first sampling s from ξ_{π} and then a from π . An MDP \mathcal{M} is *ergodic* if for all $\pi \in \Pi_{\mathcal{M}}^{\text{ml}}$, the state space of \mathcal{M}_{π} consists of a unique aperiodic BSCC with $\xi_{\pi} = \lim_{t \rightarrow \infty} \xi_{\pi}^t(\cdot \mid s)$ for all $s \in \mathcal{S}$.

Events and functions. Let $\mathbb{C}, \mathbb{T} \subseteq \mathbf{AP}$, we define the *constrained reachability* (resp. *reachability*) event as $\text{CU}\mathbb{T} = \{s_{0:\infty}, a_{0:\infty} \mid \exists i \in \mathbb{N}, \forall j < i, s_j \in \llbracket \mathbb{C} \rrbracket \wedge s_i \in \llbracket \mathbb{T} \rrbracket\} \in \Sigma(\text{Traj}_{\mathcal{M}})$ (resp. $\diamond\mathbb{T} = \neg \text{CU}\mathbb{T}$). Safety w.r.t. a set of failure states \mathbb{T} can be expressed as a safe-constrained reachability event to a safe destination \mathbb{C} (resp. safety event) through $\neg\mathbb{T}\mathbb{U}\mathbb{C}$ (resp. $\square\neg\mathbb{T} = \text{Traj}_{\mathcal{M}} \setminus \diamond\mathbb{T}$). Let $\gamma \in [0, 1[$, $\varphi \in \{\epsilon, \text{CU}\mathbb{T}, \diamond\mathbb{T}\}$ where ϵ is the empty symbol, and $\mathcal{R}^{\mathbb{T}} = (1 - \gamma)\mathbf{1}_{\llbracket \mathbb{T} \rrbracket \times \mathcal{A}}$, the *value* obtained by running $\pi \in \Pi_{\mathcal{M}}^{\text{ml}}$ from state s in \mathcal{M} is $V_{\pi}^{\varphi}(s) = \mathbb{E}_{\pi}^{\mathcal{M}[s, \varphi]}[\sum_{t=0}^{\infty} \gamma^t \mathcal{R}(s_t, a_t)]$. It corresponds to the *expected discounted* (i) *return* when $\varphi = \epsilon$ with $\mathcal{M}[s] = \mathcal{M}_s$, (ii) *constrained reachability* when $\varphi = \text{CU}\mathbb{T}$ with $\mathcal{M}[s, \text{CU}\mathbb{T}] = \mathcal{M}_s^{\llbracket \neg \mathbb{C} \rrbracket \cup \llbracket \mathbb{T} \rrbracket} \oplus \mathcal{R}^{\mathbb{T}}$, (iii) *reachability* when $\varphi = \diamond\mathbb{T}$ with $\mathcal{M}[s, \diamond\mathbb{T}] = \mathcal{M}_s^{\llbracket \mathbb{T} \rrbracket} \oplus \mathcal{R}^{\mathbb{T}}$. When $\varphi \in \{\text{CU}\mathbb{T}, \diamond\mathbb{T}\}$, observe that $V_{\pi}^{\varphi}(t) = 1$ for $t \in \llbracket \mathbb{T} \rrbracket$ and $\lim_{\gamma \rightarrow 1} V_{\pi}^{\varphi}(s) = \mathbb{P}_{\pi}^{\mathcal{M}_s}(\varphi)$ for $s \in \mathcal{S}$. The *action-value function* is $Q_{\pi}^{\varphi}(s, a) = \mathcal{R}'(s, a) + \mathbb{E}_{s' \sim \mathbf{P}(\cdot \mid s, a)}[\gamma V_{\pi}^{\varphi}(s')]$, with $\mathcal{R}' = \mathcal{R}$ if $\varphi = \epsilon$ and $\mathcal{R}' = \mathcal{R}^{\mathbb{T}}$ otherwise.

3 Latent Space Models

Given the original (continuous, possibly unknown) environment modeled as an MDP, a *latent space model* is another (simpler, smaller, and explicit) MDP with state-action space linked to the original one via *embedding functions*. The latter can be learned to optimize an *equivalence criterion* between the two models. Formally, fix MDPs $\mathcal{M} = \langle \mathcal{S}, \mathcal{A}, \mathbf{P}, \mathcal{R}, \ell, \mathbf{AP}, s_I \rangle$ and $\bar{\mathcal{M}} = \langle \bar{\mathcal{S}}, \bar{\mathcal{A}}, \bar{\mathbf{P}}, \bar{\mathcal{R}}, \bar{\ell}, \mathbf{AP}, \bar{s}_I \rangle$ such that $\bar{\mathcal{S}}$ is equipped with metric $d_{\bar{\mathcal{S}}}$. Let $\phi: \mathcal{S} \rightarrow \bar{\mathcal{S}}$ and $\psi: \mathcal{S} \times \bar{\mathcal{A}} \rightarrow \mathcal{A}$ be respectively state and action embedding functions. We refer to $\langle \bar{\mathcal{M}}, \phi, \psi \rangle$ as a latent space model of \mathcal{M} and $\bar{\mathcal{M}}$ as its *latent MDP*. We write $\bar{\Pi}^{\text{ml}} = \Pi_{\bar{\mathcal{M}}}^{\text{ml}}$, and $\bar{Q}_{\bar{\pi}}$ for the action-value function of a policy $\bar{\pi} \in \bar{\Pi}^{\text{ml}}$ in $\bar{\mathcal{M}}$. We also consider $\bar{\pi}$ as a policy in \mathcal{M} : states passed to $\bar{\pi}$ are embedded with ϕ , then actions executed are embedded with ψ . Let $\bar{\pi} \in \bar{\Pi}^{\text{ml}}$ and $s \in \mathcal{S}$, we write $\bar{a} \sim \bar{\pi}(\cdot | s)$ for $\bar{a} \sim \bar{\pi}(\cdot | \phi(s))$ and $Q_{\bar{\pi}}(s, \bar{a})$ as shorthand for $Q_{\bar{\pi}}(s, \psi(s, \bar{a}))$.

A particular point of interest is to focus on discrete latent models, where $d_{\bar{\mathcal{S}}} = \mathbf{1}_{\neq}$. In the following, we adopt the latent space model formalism of Gelada et al. (2019).

Notations. Let $\bar{\pi} \in \bar{\Pi}^{\text{ml}}$, we write $|\bar{\mathcal{R}}_{\bar{\pi}}^*|$ for $\sup_{\bar{s} \in \bar{\mathcal{S}}} |\bar{\mathcal{R}}_{\bar{\pi}}(\bar{s})|$. We say that $\bar{\mathcal{M}}$ is $\langle K_{\bar{\mathcal{R}}}^{\bar{\pi}}, K_{\bar{\mathbf{P}}}^{\bar{\pi}} \rangle$ -Lipschitz if for all $\bar{s}_1, \bar{s}_2 \in \bar{\mathcal{S}}$,

$$\begin{aligned} |\bar{\mathcal{R}}_{\bar{\pi}}(\bar{s}_1) - \bar{\mathcal{R}}_{\bar{\pi}}(\bar{s}_2)| &\leq K_{\bar{\mathcal{R}}}^{\bar{\pi}} d_{\bar{\mathcal{S}}}(\bar{s}_1, \bar{s}_2), \\ W_{d_{\bar{\mathcal{S}}}}(\bar{\mathbf{P}}_{\bar{\pi}}(\cdot | \bar{s}_1), \bar{\mathbf{P}}_{\bar{\pi}}(\cdot | \bar{s}_2)) &\leq K_{\bar{\mathbf{P}}}^{\bar{\pi}} d_{\bar{\mathcal{S}}}(\bar{s}_1, \bar{s}_2). \end{aligned}$$

Local losses. Let $\xi \in \mathcal{P}(\mathcal{S} \times \mathcal{A})$, *local losses* are defined as:

$$\begin{aligned} L_{\bar{\mathcal{R}}}^{\xi} &= \mathbb{E}_{s, \bar{a} \sim \xi} |\mathcal{R}(s, \bar{a}) - \bar{\mathcal{R}}(\phi(s), \bar{a})|, \\ L_{\bar{\mathbf{P}}}^{\xi} &= \mathbb{E}_{s, \bar{a} \sim \xi} W_{d_{\bar{\mathcal{S}}}}(\phi\mathbf{P}(\cdot | s, \bar{a}), \bar{\mathbf{P}}(\cdot | \phi(s), \bar{a})) \end{aligned}$$

where (i) $\mathcal{R}(s, \bar{a})$, (ii) $\mathbf{P}(\cdot | s, \bar{a})$, and (iii) $\phi\mathbf{P}(\cdot | s, \bar{a})$ are shorthand for (i) $\mathcal{R}(s, \psi(s, \bar{a}))$, (ii) $\mathbf{P}(\cdot | s, \psi(s, \bar{a}))$, and (iii) the distribution over $\bar{\mathcal{S}}$ of sampling $s' \sim \mathbf{P}(\cdot | s, \bar{a})$ and then embedding $\bar{s}' = \phi(s)$.

Assuming $\bar{\mathcal{M}}$ is discrete, all $W_{d_{\bar{\mathcal{S}}}}$ terms can be replaced by d_{TV} since Wasserstein coincides with TV when using the discrete metric. In that case, (optimal) constants $K_{\bar{\mathcal{R}}}^{\bar{\pi}}$ and $K_{\bar{\mathbf{P}}}^{\bar{\pi}}$ can be computed in polynomial time in $\bar{\mathcal{M}}$ for any $\bar{\pi} \in \bar{\Pi}^{\text{ml}}$.

Henceforth, we make the following assumptions.

Assumption 3.1. *MDP \mathcal{M} is ergodic.*

Assumption 3.2. *Rewards of \mathcal{M} are scaled in the interval $[-\frac{1}{2}, \frac{1}{2}]$, i.e., $\mathcal{R}: \mathcal{S} \times \mathcal{A} \rightarrow [-\frac{1}{2}, \frac{1}{2}]$.*

Assumption 3.3. *The embedding function preserves the labels, i.e., $\phi(s) = \bar{s} \implies \ell(s) = \bar{\ell}(\bar{s})$ for $s \in \mathcal{S}$, $\bar{s} \in \bar{\mathcal{S}}$.*

Seemingly restrictive at first glance, Assumption 3.1 is compliant with RL environments and a wide range of continuous learning tasks (every episodic RL process is ergodic, see Huang 2020). Discarding it restricts the upcoming guarantees to BSCCs. Assumption 3.2 basically requires rewards to be bounded and re-scalable in this interval. This is a reasonable assumption in practice and re-scaling is straightforward if bounds are known (otherwise, dynamical re-scaling is still feasible but complicates the implementation).

In Sect. 4.2, we show that Assumption 3.3 can be made trivial. Note that our approach requires Assumption 3.2 and 3.3.

Proofs of the claims made in the following two subsections are provided in supplementary material (Appendix B).

3.1 Bisimulation and Value Difference Bounds

We aim now at formally checking whether the latent space model offers a good abstraction of the original MDP \mathcal{M} . To do so, we present bounds that link the two MDPs. We extend the bounds from Gelada et al. (2019) to discrete spaces while additionally taking into account state labels and discounted reachability events. Moreover, we present new *bisimulation* bounds in the local setting.

Bisimulation. A (*probabilistic*) *bisimulation* is a behavioral equivalence between states. Formally, a bisimulation on \mathcal{M} is an equivalence relation B_{Φ} such that for all $s_1, s_2 \in \mathcal{S}$ and $\Phi \subseteq \{\mathcal{R}, \ell\}$, $s_1 B_{\Phi} s_2$ iff $\mathbf{P}(T | s_1, a) = \mathbf{P}(T | s_2, a)$, $\ell(s_1) = \ell(s_2)$ if $\ell \in \Phi$, and $\mathcal{R}(s_1, a) = \mathcal{R}(s_2, a)$ if $\mathcal{R} \in \Phi$, for each action $a \in \mathcal{A}$ and (Borel measurable) equivalence class $T \in \mathcal{S}/B_{\Phi}$. Properties of bisimulation include trace, trajectory, and value equivalence (Larsen and Skou 1989; Givan, Dean, and Greig 2003). The relation can be extended to compare two MDPs (in our case \mathcal{M} and $\bar{\mathcal{M}}$) by considering the disjoint union of their state space. We denote the largest bisimulation relation by \sim_{Φ} .

Pseudometrics. Desharnais et al. (2004) introduced *bisimulation pseudometrics* for continuous Markov processes, generalizing the notion of bisimilarity by assigning a *bisimilarity distance* between states. A *pseudometric* \tilde{d} satisfies symmetry and the triangle inequality.

Probabilistic bisimilarity can be characterized by a logical family of functional expressions derived from a logic \mathcal{L} . More specifically, given a policy $\pi \in \Pi_{\mathcal{M}}^{\text{ml}}$, we consider a family $\mathcal{F}_{\gamma}^{\mathcal{L}}(\pi)$ of real-valued functions f , parameterized by the discount factor γ and defining the semantics of \mathcal{L} in \mathcal{M}_{π} . Such a logic allows formalizing discounted properties, including reachability (e.g., Chatterjee et al. 2008). The related pseudometric \tilde{d}_{π} is defined as: $\tilde{d}_{\pi}(s_1, s_2) = \sup_{f \in \mathcal{F}_{\gamma}^{\mathcal{L}}(\pi)} |f(s_1) - f(s_2)|$, for all $s_1, s_2 \in \mathcal{S}$. We distinguish between pseudometrics $\tilde{d}_{\pi}^{\mathcal{R}}$, characterized by functional expressions including rewards (e.g., Ferns, Precup, and Knight 2014), and \tilde{d}_{π}^{ℓ} , whose functional expressions are based on state labels (e.g., Chen, van Breugel, and Worrell 2012). Let \tilde{P} be the space of pseudometrics on \mathcal{S} and $\varphi \in \{\mathcal{R}, \ell\}$. Define $\Delta: \tilde{P} \rightarrow \tilde{P}$ so that $\Delta(\tilde{d}_{\pi}^{\varphi})(s_1, s_2)$ is $(1 - \gamma) |\mathcal{R}_{\pi}(s_1) - \mathcal{R}_{\pi}(s_2)| \cdot \mathbf{1}_{\{\mathcal{R}\}}(\varphi) + M$ where:

$$M = \max \left\{ \gamma W_{d_{\bar{\mathcal{S}}}}(\mathbf{P}_{\pi}(\cdot | s_1), \mathbf{P}_{\pi}(\cdot | s_2)), \mathbf{1}_{\neq}(\ell(s_1), \ell(s_2)) \cdot \mathbf{1}_{\{\ell\}}(\varphi) \right\},$$

then $\tilde{d}_{\pi}^{\varphi}$ is its unique fixed point whose kernel is $\sim_{\{\varphi\}}$, i.e., $\tilde{d}_{\pi}^{\varphi}(s_1, s_2) = 0$ iff $s_1 \sim_{\{\varphi\}} s_2$ (van Breugel and Worrell 2001; Ferns, Precup, and Knight 2014), and $|V_{\pi}(s_1) - V_{\pi}(s_2)| \leq \tilde{d}_{\pi}^{\mathcal{R}}(s_1, s_2)/1 - \gamma$ (Ferns, Panagaden, and Precup 2005).

Bisimulation bounds. While computing this distance is intractable in practice, especially when continuous spaces are

involved, we emphasize that local losses can be used to evaluate the original and latent model bisimilarity. Fix $\bar{\pi} \in \bar{\Pi}^{\text{ml}}$ and assume \mathcal{M} is discrete. Given the induced stationary distribution $\xi_{\bar{\pi}}$ in \mathcal{M} ,

$$\begin{aligned} \mathbb{E}_{s \sim \xi_{\bar{\pi}}} \tilde{d}_{\bar{\pi}}^{\mathcal{R}}(s, \phi(s)) &\leq L_{\mathcal{R}}^{\xi_{\bar{\pi}}} + \gamma L_{\mathbf{P}}^{\xi_{\bar{\pi}}} \frac{K_{\mathcal{R}}^{\bar{\pi}}}{1 - \gamma K_{\mathbf{P}}^{\bar{\pi}}}, \\ \mathbb{E}_{s \sim \xi_{\bar{\pi}}} \tilde{d}_{\bar{\pi}}^{\ell}(s, \phi(s)) &\leq \frac{\gamma L_{\mathbf{P}}^{\xi_{\bar{\pi}}}}{1 - \gamma}, \end{aligned} \quad (1)$$

where $\bar{\mathcal{M}}$ is $\langle K_{\mathcal{R}}^{\bar{\pi}}, K_{\mathbf{P}}^{\bar{\pi}} \rangle$ -Lipschitz. The result provides us a general way to assess the quality of the abstraction: the bisimulation distance between states and their embedding is guaranteed to be small in average whenever local losses are small. Analogously, local losses can further be used to check whether two states with the same representation are indeed bisimilarly close: for $s_1, s_2 \in \mathcal{S}$ with $\phi(s_1) = \phi(s_2)$,

$$\begin{aligned} \tilde{d}_{\bar{\pi}}^{\mathcal{R}}(s_1, s_2) &\leq \left[L_{\mathcal{R}}^{\xi_{\bar{\pi}}} + \frac{\gamma L_{\mathbf{P}}^{\xi_{\bar{\pi}}} K_{\mathcal{R}}^{\bar{\pi}}}{1 - \gamma K_{\mathbf{P}}^{\bar{\pi}}} \right] (\xi_{\bar{\pi}}^{-1}(s_1) + \xi_{\bar{\pi}}^{-1}(s_2)), \\ \tilde{d}_{\bar{\pi}}^{\ell}(s_1, s_2) &\leq \frac{\gamma L_{\mathbf{P}}^{\xi_{\bar{\pi}}}}{1 - \gamma} (\xi_{\bar{\pi}}^{-1}(s_1) + \xi_{\bar{\pi}}^{-1}(s_2)). \end{aligned} \quad (2)$$

Remark 1. Our goal is to quantify the gap between the behaviors induced by the latent policy executed in the original environment compared to those induced when executed in the latent MDP. This allows for example to lift the guarantees obtained by model-checking $\bar{\mathcal{M}}_{\bar{\pi}}$ to $\mathcal{M}_{\bar{\pi}}$. For this reason, notice that the expectations of Eq. 1 are set over states produced by $\bar{\pi}$ in the original environment: this way, states that are likely to be seen under $\bar{\pi}$ in \mathcal{M} are ensured to have this behavioral gap bounded by a factor of $L_{\mathcal{R}}^{\xi_{\bar{\pi}}}$ and/or $L_{\mathbf{P}}^{\xi_{\bar{\pi}}}$.

Value difference bounds. Considering discounted returns or a specific event, the quality of the latent abstraction can be in particular formalized by means of *value difference bounds*. These bounds can be intuitively derived by taking the value function as a real-valued function from $\mathcal{F}_{\gamma}^{\mathcal{L}}(\pi)$. Let $\mathbf{C}, \mathbf{T} \subseteq \mathbf{AP}$, $\varphi \in \{\text{CUT}, \diamond \mathbf{T}\}$ and $K_{\bar{\mathcal{V}}} = \min(|\bar{\mathcal{R}}_{\bar{\pi}}^*|/1 - \gamma, K_{\bar{\mathcal{R}}}^{\bar{\pi}}/1 - \gamma K_{\mathbf{P}}^{\bar{\pi}})$, then,

$$\begin{aligned} \mathbb{E}_{s, \bar{a} \sim \xi_{\bar{\pi}}} |Q_{\bar{\pi}}(s, \bar{a}) - \bar{Q}_{\bar{\pi}}(\phi(s), \bar{a})| &\leq \frac{L_{\mathcal{R}}^{\xi_{\bar{\pi}}} + \gamma K_{\bar{\mathcal{V}}} L_{\mathbf{P}}^{\xi_{\bar{\pi}}}}{1 - \gamma}, \\ \mathbb{E}_{s, \bar{a} \sim \xi_{\bar{\pi}}} |Q_{\bar{\pi}}^{\varphi}(s, \bar{a}) - \bar{Q}_{\bar{\pi}}^{\varphi}(\phi(s), \bar{a})| &\leq \frac{\gamma L_{\mathbf{P}}^{\xi_{\bar{\pi}}}}{1 - \gamma}. \end{aligned} \quad (3)$$

Moreover, for any states $s_1, s_2 \in \mathcal{S}$ with $\phi(s_1) = \phi(s_2)$,

$$\begin{aligned} |V_{\bar{\pi}}(s_1) - V_{\bar{\pi}}(s_2)| &\leq \frac{L_{\mathcal{R}}^{\xi_{\bar{\pi}}} + \gamma K_{\bar{\mathcal{V}}} L_{\mathbf{P}}^{\xi_{\bar{\pi}}}}{1 - \gamma} (\xi_{\bar{\pi}}^{-1}(s_1) + \xi_{\bar{\pi}}^{-1}(s_2)), \\ |V_{\bar{\pi}}^{\varphi}(s_1) - V_{\bar{\pi}}^{\varphi}(s_2)| &\leq \frac{\gamma L_{\mathbf{P}}^{\xi_{\bar{\pi}}}}{1 - \gamma} (\xi_{\bar{\pi}}^{-1}(s_1) + \xi_{\bar{\pi}}^{-1}(s_2)). \end{aligned} \quad (4)$$

Intuitively, when local losses are sufficiently small, then (i) the value difference of states and their embedding that are likely to be seen under a latent policy is also small, and (ii) states with the same embedding have close values.

3.2 Checking the Quality of the Abstraction

While bounding the difference between values offered by $\bar{\pi} \in \bar{\Pi}^{\text{ml}}$ in \mathcal{M} and $\bar{\mathcal{M}}$ is theoretically possible using $L_{\mathcal{R}}^{\xi_{\bar{\pi}}}$ and $L_{\mathbf{P}}^{\xi_{\bar{\pi}}}$, we need to accurately approximate these losses from samples to further offer practical guarantees (recall that \mathcal{M} is unknown). Although the agent is able to produce execution traces by interacting with \mathcal{M} , estimating the expectation over the Wasserstein is intractable. Intuitively, even if approximating Wasserstein from samples is possible (e.g., Genevay et al. 2019), this would require access to a generative model for $\mathbf{P}(\cdot | s, a)$ (e.g., Kearns, Mansour, and Ng 2002) from which we would have to draw a sufficient number of samples for each s, a drawn from $\xi_{\bar{\pi}}$ to then be able to estimate the expectation. Gelada et al. (2019) overcome this issue by assuming a deterministic MDP, which allows optimizing an approximation of $L_{\mathbf{P}}^{\xi_{\bar{\pi}}}$ through gradient descent. To deal with general MDPs, we study an upper bound on $L_{\mathbf{P}}^{\xi_{\bar{\pi}}}$ that can be efficiently approximated from samples:

$$L_{\mathbf{P}}^{\xi_{\bar{\pi}}} \leq \mathbb{E}_{s, \bar{a}, s' \sim \xi_{\bar{\pi}}} W_{d_{\bar{\mathcal{S}}}}(\phi(\cdot | s'), \bar{\mathbf{P}}(\cdot | \phi(s), \bar{a})) = \hat{L}_{\mathbf{P}}^{\xi_{\bar{\pi}}},$$

where $\xi_{\bar{\pi}}(s, \bar{a}, s') = \xi_{\bar{\pi}}(s, \bar{a}) \cdot \mathbf{P}(s' | s, \bar{a})$ and $\phi(\bar{s} | s) = \mathbf{1}_{=(\phi(s), \bar{s})}$. We now provide *probably approximately correct* (PAC) guarantees for estimating local losses for discrete latent models, derived from the Hoeffding's inequalities.

Lemma 3.4. *Suppose $\bar{\mathcal{M}}$ is discrete and the agent interacts with \mathcal{M} by executing $\bar{\pi} \in \bar{\Pi}$, thus producing $\langle s_{0:T}, \bar{a}_{0:T-1}, r_{0:T-1} \rangle \sim \xi_{\bar{\pi}}$. Let $\varepsilon, \delta \in]0, 1[$ and denote by*

$$\begin{aligned} \hat{L}_{\mathcal{R}}^{\xi_{\bar{\pi}}} &= \frac{1}{T} \sum_{t=0}^{T-1} |r_t - \bar{\mathcal{R}}(\phi(s_t), \bar{a}_t)|, \\ \hat{L}_{\mathbf{P}}^{\xi_{\bar{\pi}}} &= \frac{1}{T} \sum_{t=0}^{T-1} [1 - \bar{\mathbf{P}}(\phi(s_{t+1}) | \phi(s_t), \bar{a}_t)]. \end{aligned}$$

Then after $T \geq \lceil -\log(\frac{\delta}{4})/2\varepsilon^2 \rceil$ steps, $|L_{\mathcal{R}}^{\xi_{\bar{\pi}}} - \hat{L}_{\mathcal{R}}^{\xi_{\bar{\pi}}}| \leq \varepsilon$ and $|\hat{L}_{\mathbf{P}}^{\xi_{\bar{\pi}}} - \hat{L}_{\mathbf{P}}^{\xi_{\bar{\pi}}}| \leq \varepsilon$ with probability at least $1 - \delta$.

This yields the following Theorem, finally allowing to check the abstraction quality as a bounded value difference.

Theorem 3.5. *Let $\bar{\pi} \in \bar{\Pi}^{\text{ml}}$ and assume $\bar{\mathcal{M}}$ is discrete and $\langle K_{\mathcal{R}}^{\bar{\pi}}, K_{\mathbf{P}}^{\bar{\pi}} \rangle$ -Lipschitz. Let $\mathbf{C}, \mathbf{T} \subseteq \mathbf{AP}$, $\varphi \in \{\text{CUT}, \diamond \mathbf{T}\}$, and $K_{\bar{\mathcal{V}}} = \min(|\bar{\mathcal{R}}_{\bar{\pi}}^*|/1 - \gamma, K_{\bar{\mathcal{R}}}^{\bar{\pi}}/1 - \gamma K_{\mathbf{P}}^{\bar{\pi}})$. Let $\varepsilon, \delta \in]0, 1[$ and $\xi_{\bar{\pi}}$ be the stationary distribution of $\mathcal{M}_{\bar{\pi}}$. Then, after $T \geq \lceil -\log(\frac{\delta}{4})(1 + \gamma K_{\bar{\mathcal{V}}})^2/2\varepsilon^2(1 - \gamma)^2 \rceil$ interaction steps through $\xi_{\bar{\pi}}$,*

$$\begin{aligned} \mathbb{E}_{s, \bar{a} \sim \xi_{\bar{\pi}}} |Q_{\bar{\pi}}(s, \bar{a}) - \bar{Q}_{\bar{\pi}}(\phi(s), \bar{a})| &\leq \frac{\hat{L}_{\mathcal{R}}^{\xi_{\bar{\pi}}} + \gamma K_{\bar{\mathcal{V}}} \hat{L}_{\mathbf{P}}^{\xi_{\bar{\pi}}}}{1 - \gamma} + \varepsilon, \\ \mathbb{E}_{s, \bar{a} \sim \xi_{\bar{\pi}}} |Q_{\bar{\pi}}^{\varphi}(s, \bar{a}) - \bar{Q}_{\bar{\pi}}^{\varphi}(\phi(s), \bar{a})| &\leq \frac{\gamma \hat{L}_{\mathbf{P}}^{\xi_{\bar{\pi}}}}{1 - \gamma} + \frac{\gamma \varepsilon}{1 + \gamma K_{\bar{\mathcal{V}}}} \end{aligned}$$

with probability at least $1 - \delta$.

4 Variational Markov Decision Processes

We now provide a framework based on *variational autoencoders* (Kingma and Welling 2014) that allows us to learn a discrete latent space model of \mathcal{M} through the interaction of the agent executing a pre-learned RL policy $\pi \in \Pi_{\mathcal{M}}^{\text{ml}}$ with the environment. Concretely, we seek a discrete latent space model $\langle \bar{\mathcal{M}}_{\theta}, \phi_{\iota}, \psi_{\iota, \theta} \rangle$ such that $\bar{\mathcal{M}}_{\theta} = \langle \bar{\mathcal{S}}, \bar{\mathcal{A}}, \bar{\mathbf{P}}_{\theta}, \bar{\mathcal{R}}_{\theta}, \bar{\ell}_{\theta}, \mathbf{A}\mathbf{P}, \bar{s}_I \rangle$. We propose to learn the parameters $\langle \iota, \theta \rangle$ of an *encoder* Q_{ι} and a *behavioral model* P_{θ} from which we can retrieve (i) the embedding functions ϕ_{ι} and $\psi_{\iota, \theta}$, (ii) the latent MDP components $\bar{\mathbf{P}}_{\theta}$, $\bar{\mathcal{R}}_{\theta}$, and $\bar{\ell}_{\theta}$, and (iii) a latent policy $\bar{\pi}_{\theta} \in \bar{\Pi}^{\text{ml}}$, via $\min_{\theta} D(\mathcal{M}_{\pi}, P_{\theta})$, where D is a discrepancy measure. Intuitively, the end goal is to learn (i) a discrete representation of \mathcal{S} and \mathcal{A} (ii) to mimic the behaviors of the original MDP over the induced latent spaces, thus yielding a latent MDP with a bisimulation distance close to \mathcal{M} , and (iii) to *distill* π into $\bar{\pi}_{\theta}$. In the following, we distinguish the case where we only learn $\bar{\mathcal{S}}$, with $\bar{\mathcal{A}} = \mathcal{A}$ (in that case, \mathcal{A} is assumed to be discrete), and the one where we additionally need to discretize the set of actions and learn $\bar{\mathcal{A}}$.

4.1 Evidence Lower Bound

In this work, we focus on the case where D_{KL} is used as discrepancy measure: the goal is optimizing $\min_{\theta} D_{\text{KL}}(\mathcal{M}_{\pi} \parallel P_{\theta})$ or equivalently maximizing the marginal *log-likelihood of traces* of \mathcal{M} , i.e., $\mathbb{E}_{\hat{\tau} \sim \mathcal{M}_{\pi}} [\log P_{\theta}(\hat{\tau})]$, where

$$P_{\theta}(\hat{\tau}) = \int_{\text{Traj}_{\bar{\mathcal{M}}_{\theta}}} P_{\theta}(\hat{\tau} \mid z_{0:T}) d\bar{\mathbf{P}}_{\bar{\pi}_{\theta}}(z_{0:T}), \quad (5)$$

$\hat{\tau} = \langle s_{0:T}, a_{0:T-1}, r_{0:T-1}, l_{0:T} \rangle$, $z \in \mathcal{Z}$ with $\mathcal{Z} = \bar{\mathcal{S}}$ if $\bar{\mathcal{A}} = \mathcal{A}$ and $\mathcal{Z} = \bar{\mathcal{S}} \times \bar{\mathcal{A}}$ otherwise, $\bar{\mathbf{P}}_{\bar{\pi}_{\theta}}(\bar{s}_{0:T}) = \prod_{t=0}^{T-1} \bar{\mathbf{P}}_{\bar{\pi}_{\theta}}(\bar{s}_{t+1} \mid \bar{s}_t)$, and $\bar{\mathbf{P}}_{\bar{\pi}_{\theta}}(\bar{s}_{0:T}, \bar{a}_{0:T-1}) = \prod_{t=0}^{T-1} \bar{\pi}_{\theta}(\bar{a}_t \mid \bar{s}_t) \cdot \bar{\mathbf{P}}_{\theta}(\bar{s}_{t+1} \mid \bar{s}_t, \bar{a}_t)$. The dependency of $\hat{\tau}$ on \mathcal{Z} in Eq. 5 is made explicit by the law of total probability.

Optimizing $\mathbb{E}_{\hat{\tau} \sim \mathcal{M}_{\pi}} [\log P_{\theta}(\hat{\tau})]$ through Eq. 5 is typically intractable (Kingma and Welling 2014). To overcome this, we use an encoder $Q_{\iota}(z_{0:T} \mid \hat{\tau})$ to set up a *lower bound* on the log-likelihood of produced traces, often referred to as *evidence lower bound* (ELBO, Hoffman et al. 2013):

$$\begin{aligned} & \log P_{\theta}(\hat{\tau}) - D_{\text{KL}}(Q_{\iota}(\cdot \mid \hat{\tau}) \parallel P_{\theta}(\cdot \mid \hat{\tau})) \\ &= \mathbb{E}_{z_{0:T} \sim Q_{\iota}(\cdot \mid \hat{\tau})} [\log P_{\theta}(\hat{\tau} \mid z_{0:T})] - D_{\text{KL}}(Q_{\iota}(\cdot \mid \hat{\tau}) \parallel \bar{\mathbf{P}}_{\bar{\pi}_{\theta}}). \end{aligned}$$

The purpose of optimizing the ELBO is twofold. First, this allows us learning ϕ_{ι} via (i) $Q_{\iota}(\bar{s}_{0:T} \mid \hat{\tau}) = \prod_{t=0}^{T-1} \phi_{\iota}(\bar{s}_t \mid s_t)$ or (ii) $Q_{\iota}(\bar{s}_{0:T}, \bar{a}_{0:T-1} \mid \hat{\tau}) = Q_{\iota}(\bar{a}_{0:T-1} \mid \bar{s}_{0:T}, \hat{\tau}) \cdot Q_{\iota}(\bar{s}_{0:T} \mid \hat{\tau})$, where $Q_{\iota}(\bar{a}_{0:T-1} \mid \bar{s}_{0:T}, \hat{\tau}) = \prod_{t=0}^{T-1} Q_{\iota}^{\mathcal{A}}(\bar{a}_t \mid \bar{s}_t, a_t)$, $Q_{\iota}^{\mathcal{A}}$ being an action encoder. We assume here that encoding states and actions to latent spaces is independent of rewards. We additionally make them independent of $l_{0:T}$ by assuming that ℓ is known. This allows ϕ_{ι} to encode states and their labels directly into the latent space (cf. Sect. 4.2).

Second, we assume the existence of latent reward and label models, i.e., $P_{\theta}^{\mathcal{R}}$ and P_{θ}^{ℓ} , allowing to recover respectively

$\bar{\mathcal{R}}_{\theta}$ and $\bar{\ell}_{\theta}$, as well as a *generative model* $P_{\theta}^{\mathcal{G}}$, enabling the reconstruction of states and actions. This allows decomposing the behavioral model P_{θ} into:

$$\begin{aligned} & P_{\theta}(s_{0:T}, a_{0:T-1}, r_{0:T-1}, l_{0:T} \mid z_{0:T}) \\ &= P_{\theta}^{\mathcal{G}}(s_{0:T} \mid \bar{s}_{0:T}) \cdot P_{\theta}^{\mathcal{G}}(a_{0:T-1} \mid z_{0:T}) \\ & \quad \cdot P_{\theta}^{\mathcal{R}}(r_{0:T-1} \mid \bar{s}_{0:T}, \bar{a}_{0:T-1}) \cdot P_{\theta}^{\ell}(l_{0:T} \mid \bar{s}_{0:T}), \end{aligned}$$

where $P_{\theta}^{\mathcal{G}}(s_{0:T} \mid \bar{s}_{0:T}) = \prod_{t=0}^{T-1} P_{\theta}^{\mathcal{G}}(s_t \mid \bar{s}_t)$,

$$P_{\theta}^{\mathcal{G}}(a_{0:T-1} \mid z_{0:T-1}) = \begin{cases} \prod_{t=0}^{T-1} \bar{\pi}_{\theta}(a_t \mid \bar{s}_t) & \text{if } \bar{\mathcal{A}} = \mathcal{A} \\ \prod_{t=0}^{T-1} \psi_{\theta}(a_t \mid \bar{s}_t, \bar{a}_t) & \text{else,} \end{cases}$$

$P_{\theta}^{\mathcal{R}}(r_{0:T-1} \mid \bar{s}_{0:T}, \bar{a}_{0:T-1}) = \prod_{t=0}^{T-1} P_{\theta}^{\mathcal{R}}(r_t \mid \bar{s}_t, \bar{a}_t)$, and

$$P_{\theta}^{\ell}(l_{0:T} \mid \bar{s}_{0:T}) = \prod_{t=0}^{T-1} P_{\theta}^{\ell}(l_t \mid \bar{s}_t).$$

Model ψ_{θ} allows learning the action embedding function via $\psi_{\iota, \theta}(a \mid s, \bar{a}) = \mathbb{E}_{\bar{s} \sim \phi_{\iota}(\cdot \mid s)} \psi_{\theta}(a \mid \bar{s}, \bar{a})$ for all $s \in \mathcal{S}, a \in \mathcal{A}, \bar{a} \in \bar{\mathcal{A}}$. We also argue that a *perfect reconstruction* of labels is possible, i.e., $P_{\theta}^{\ell}(l_{0:T} \mid \bar{s}_{0:T}) = 1$, due to the labels being encoded into the latent space. From now on, we thus omit the label term.

Deterministic embedding functions ϕ_{ι} , $\psi_{\iota, \theta}$ and $\bar{\mathcal{R}}_{\theta}$ can finally be obtained by taking the mode of their distribution.

Back to the local setting. Taking Assumption 3.1 into account, drawing multiple finite traces $\hat{\tau} \sim \mathcal{M}_{\pi}$ can be seen as a continuous interaction with \mathcal{M} along an infinite trace (Huang 2020). This observation allows us to formulate the ELBO in the local setting¹ and connect to local losses:

$$\max_{\iota, \theta} \text{ELBO}(\bar{\mathcal{M}}_{\theta}, \phi_{\iota}, \psi_{\iota, \theta}) = - \min_{\iota, \theta} \{ \mathbf{D}_{\iota, \theta} + \mathbf{R}_{\iota, \theta} \},$$

where \mathbf{D} and \mathbf{R} denote respectively the *distortion* and *rate* of the variational model (Alemi et al. 2018), given by

$$\mathbf{D}_{\iota, \theta} = - \begin{cases} \mathbb{E}_{\substack{s, a, r, s' \sim \xi_{\pi} \\ \bar{s}, \bar{s}' \sim \phi_{\iota}(\cdot \mid s, s')}} [\log P_{\theta}^{\mathcal{G}}(s' \mid \bar{s}') + \log \bar{\pi}_{\theta}(a \mid \bar{s}) + \log P_{\theta}^{\mathcal{R}}(r \mid \bar{s}, a)] & \text{if } \bar{\mathcal{A}} = \mathcal{A}, \\ \mathbb{E}_{\substack{s, a, r, s' \sim \xi_{\pi} \\ \bar{s}, \bar{s}' \sim \phi_{\iota}(\cdot \mid s, s')}} [\log P_{\theta}^{\mathcal{G}}(s' \mid \bar{s}') + \log \psi_{\theta}(a \mid \bar{s}, \bar{a}) + \log P_{\theta}^{\mathcal{R}}(r \mid \bar{s}, \bar{a})] & \text{else, and} \end{cases}$$

$$\mathbf{R}_{\iota, \theta} = \begin{cases} \mathbb{E}_{\substack{s, a, s' \sim \xi_{\pi} \\ \bar{s} \sim \phi_{\iota}(\cdot \mid s)}} [D_{\text{KL}}(\phi_{\iota}(\cdot \mid s') \parallel \bar{\mathbf{P}}_{\bar{\pi}_{\theta}}(\cdot \mid \bar{s}))] & \text{if } \bar{\mathcal{A}} = \mathcal{A}, \\ \mathbb{E}_{\substack{s, a, s' \sim \xi_{\pi} \\ \bar{s} \sim \phi_{\iota}(\cdot \mid s)}} [D_{\text{KL}}(\phi_{\iota}(\cdot \mid s') \parallel \bar{\mathbf{P}}_{\theta}(\cdot \mid \bar{s}, \bar{a})) + D_{\text{KL}}(Q_{\iota}^{\mathcal{A}}(\cdot \mid \bar{s}, a) \parallel \bar{\pi}_{\theta}(\cdot \mid \bar{s}))] & \text{else.} \end{cases}$$

We omit the subscripts when the context is clear. The optimization of ELBO($\bar{\mathcal{M}}_{\theta}, \phi_{\iota}, \psi_{\iota, \theta}$) allows for an indirect optimization of the local losses through their variational versions: (i) $L_{\mathcal{R}}^{\xi_{\pi}}$ via the log-likelihood of rewards produced, and (ii) $L_{\mathbf{P}}^{\xi_{\pi}}$ where we change the Wasserstein term to the KL divergence. Note that this last change means we do not necessarily obtain the theoretical guarantees on the quality

¹The expert reader might note this is not the standard definition of ELBO, we prove in Appendix (Corollary C.1.1) that this reformulation is valid because of developments in Sect. 3.

of the abstraction via its optimization. Nevertheless, our experiments indicate KL divergence is a good proxy of the Wasserstein term in practice. In particular, in the discrete setting, Wasserstein matches TV and one can relate the proxy with the original metric using the Pinkster’s inequality.

4.2 VAE Distributions

Discrete distributions. We aim at learning *discrete* latent spaces $\bar{\mathcal{S}}$ and $\bar{\mathcal{A}}$, the distributions ϕ_ι , Q_ι^A , $\bar{\mathbf{P}}_\theta$, and $\bar{\pi}_\theta$ are thus supposed to be discrete. Two main challenges arise: (i) gradient descent is not applicable to learn ι and θ due to the discontinuity of $\bar{\mathcal{S}}$ and $\bar{\mathcal{A}}$, and (ii) sampling from these distributions must be a *derivable operation*. We overcome these by using *continuous relaxation of Bernoulli distributions* to learn a binary representation of the latent states, and the *Gumbel softmax trick* for the latent action space (Jang, Gu, and Poole 2017; Maddison, Mnih, and Teh 2017).

Labels. To enable $\log P_\theta^\ell(l_{0:T} | \bar{s}_{0:T}) = 0$, we linearly encode $\ell(s_t) = l_t$ into each \bar{s}_t via ϕ_ι . Recall that labels are binary encoded, so we allocate them $|\mathbf{AP}|$ bits in $\bar{\mathcal{S}}$. Then, $\phi_\iota(\bar{s} | s) > 0$ implies $\ell(s) = \bar{\ell}_\theta(\bar{s})$, for all $s \in \mathcal{S}$, $\bar{s} \in \bar{\mathcal{S}}$, satisfying Assumption 3.3 if ϕ_ι is deterministic.

Decoders. For P_θ^G , ψ_θ , and P_θ^R , we learn the parameters of multivariate normal distributions. This further allows linking all $\bar{s} \in \bar{\mathcal{S}}$ to the parameters of $P_\theta^G(\cdot | \bar{s})$ for explainability.

4.3 Posterior Collapse

A common issue encountered while optimizing variational models via the ELBO is *posterior collapse*. Intuitively, this results in a degenerate local optimum where the model learns to ignore the latent space. With a discrete encoder, this translates into a deterministic mapping to a single latent state, regardless of the input. From an information-theoretic point of view, optimizing the ELBO gives way to a trade-off between the minimization of \mathbf{R} and \mathbf{D} , where the feasible region is a convex set (Alemi et al. 2018). Posterior collapse occurs when $\mathbf{R} \approx 0$ (*auto-decoding limit*). On the other hand, one can achieve $\mathbf{D} \approx 0$ (*auto-encoding limit*) at the price of a higher rate.

Regularization terms. Various solutions have been proposed in the literature to prevent posterior collapse. They include *entropy regularization* (via $\alpha \in [0, \infty]$, e.g., Burke, Hristov, and Ramamoorthy 2019; Dong et al. 2020) and *KL-scaling* (via $\beta \in [0, 1]$, e.g., Alemi et al. 2018), consisting in changing ELBO to $\langle \alpha, \beta \rangle$ -ELBO = $-(\mathbf{D} + \beta \cdot \mathbf{R}) + \alpha \cdot H(Q_\iota)$, where $H(Q_\iota)$ denotes the entropy of an encoding distribution. We choose to measure the entropy of the *marginal* encoder, given by $Q_\iota(\bar{s}) = \mathbb{E}_{s \sim \xi_\pi} \phi_\iota(\bar{s} | s)$. Intuitively, this encourages the encoder to learn to make plenty use of the latent space. The parameter β allows to interpolate between auto-encoding and auto-decoding behavior, which is not possible with the standard ELBO objective.

A drawback of these methods is that we no longer optimize a lower bound on the log-likelihood of the input while optimizing $\langle \alpha, \beta \rangle$ -ELBO. In practice, setting up annealing schemes for α and β allows to eventually recover ELBO and avoid posterior collapse ($\alpha = 0$ and $\beta = 1$ matches ELBO).

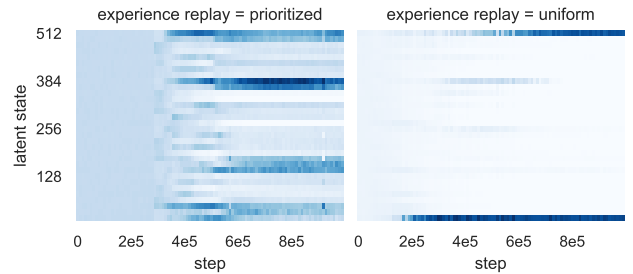


Figure 1: Latent space distribution along training steps for the CartPole environment. The intensity of the blue hue corresponds to the frequency of latent states produced by ϕ_ι during training. We compare a bucket-based prioritized against a simple uniform experience replay. The latent space learned via the uniform buffer collapses to two latent states.

Prioritized replay buffers. To enable meaningful use of latent space to represent input state-actions pairs, Q_ι should learn to (i) exploit the entire latent space, and (ii) encode wisely states and actions of transitions yielding poor ELBO, being generally sensitive to bad representation embedding. This motivates us to use a *prioritized replay buffer* (Schaul et al. 2016) to store transitions and sample them when optimizing ELBO. Draw $\langle s, a, r, s' \rangle \sim \xi_\pi$ and let $p_{\langle s, a, r, s' \rangle}$ be its priority, we introduce the following priority functions.

- *Bucket-based priority:* we partition the buffer in $|\bar{\mathcal{S}}|$ buckets. Let $N \in \mathbb{N}$ and $b: \bar{\mathcal{S}} \rightarrow \mathbb{N}$ be respectively step and latent state counters. At each step, let $\bar{s} \sim \phi_\iota(\cdot | s)$, we assign $p_{\langle s, a, r, s' \rangle}$ to $N/b(\bar{s})$, then increment N and $b(\bar{s})$ of one. This allows ϕ_ι to process states being infrequently visited under π and learn to fairly distribute $\bar{\mathcal{S}}$.
- *Loss-based priority:* we set $p_{\langle s, a, r, s' \rangle}$ to its individual transition loss, which enables to learn improving the representation of states and actions that yield poor ELBO.

5 Experiments

The goal of our experiments² is to evaluate the quality of the latent space model learned and the policy distilled via our VAE-MDP framework. This evaluation consists of: an analysis of the training of the latent space model and the benefits of our method to avoid posterior collapse, assessing the quality of the abstraction learned via PAC local losses bounds, and testing the performance of the distilled policy. This allows to assess if the latent model learned yields a sound compression of the state-action space that retains the necessary information to optimize the return. We evaluate our method on classic OpenAI environments (Brockman et al. 2016) with (i) continuous states and discrete actions (CartPole, MountainCar, and Acrobot), and (ii) where both, states and actions, are continuous (Pendulum and LunarLander). We distill RL policies π learned via DQN (Mnih et al. 2015) for case (i), and SAC (Haarnoja et al. 2018) for case (ii). The

²The code for conducting the experiments is available at https://github.com/florentdelgrange/vae_mdp

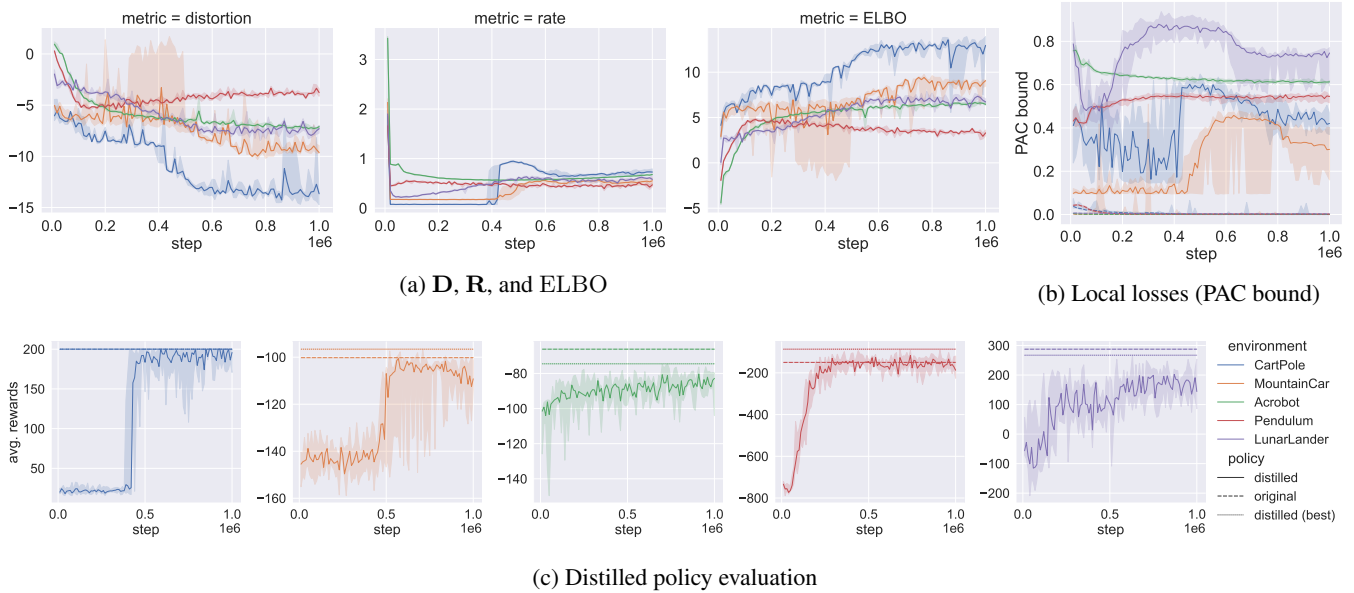


Figure 2: Plots reporting (2a) **D**, **R**, and ELBO (approximated over a large batch sampled from the replay buffer, using discrete latent distributions and averaged using importance sampling weights), (2b) PAC local losses approximation for $\varepsilon = 10^{-2}$, $\delta = 5 \cdot 10^{-3}$: solid lines stand for the transition loss and dashed lines for the reward loss, and (2c) the expected episode return (approximated by averaging over 30 episodes). For each environment, we train five different instances of our VAE with different random seeds, where the solid line corresponds to the median and the shaded interval to the interquartile range.

exact setting and labeling functions used to reproduce our results are provided in supplementary material (Appendix E).

Latent spaces. Since latent spaces are trained to enable formal verification, we choose $\log_2 |\mathcal{S}|$ and $|\mathcal{A}|$ ranging from 9 bits and 2 actions (coarser) to 16 bits and 5 actions (finer) to make them tractable for model checkers — see Budde et al. (2020) for a performance comparison of modern tools for a range of instances with large model size. Depending on the property to verify, the latent space may have to be finer since (i) we need to reserve $|\mathbf{AP}|$ bits in the representation of \mathcal{S} for labels, and (ii) this allows the agent to take more precise decisions over a finer partition of the latent space. We then select the model with the best trade-off between abstraction quality (measured via $\hat{L}_{\mathcal{R}}^{\xi_{\bar{\pi}_\theta}}$ and $\hat{L}_{\mathcal{P}}^{\xi_{\bar{\pi}_\theta}}$) and performance (i.e., the return approximated by running $\bar{\pi}$ in \mathcal{M}).

ELBO optimization. In order to allow ELBO to be trained efficiently, posterior collapse has to be tackled from the very first stages of training. In fact, we found that the KL-scaling and entropy regularization annealing schemes (cf. Sect. 4.3) were necessary to avoid the latent space to collapse into a single state-action pair after only a few training steps. We found the most efficient to start with an autoencoder behavior ($\beta_0 = 0$) and a large entropy regularizer (e.g., $\alpha_0 = 10$) during the 10^4 first steps, and then anneal them via $\alpha_t = \alpha_0 \cdot (1 - \tau)^t$, $\beta_t = 1 - (1 - \tau)^t$ (e.g., $\tau = 10^{-5}$) to fully recover the original ELBO in a second training phase. We also found that prioritized experience replays further prevent posterior collapse during training (cf. Fig. 1). Fig. 2a shows that training ELBO this way results in a stable learning procedure that successfully minimizes **D** while preventing an

auto-decoding behavior by keeping **R** away from 0.

Local losses. We compute the PAC local losses bounds presented in Sect. 3 along training steps (Fig. 2b). When the policy is eventually distilled (Fig. 2c) and $\bar{\pi}_\theta$ achieves performance similar to those of π , the learning curves stabilize, while maximizing ELBO successfully allows minimizing the local losses. In every environment where we tested our method, a low reward loss is maintained while the transition loss reaches values in the interval $[1/5, 3/5]$ for most of the instances. These values are thus guaranteed to upper bound the expected bisimulation distance between \mathcal{M} and $\bar{\mathcal{M}}$ as well as their value difference. We do not expect our approach to reach zero reward and transition loss though, since we pass from continuous to discrete spaces: the abstraction induced by our approach is always coarser than the original spaces, which translates in general to precision loss. This precision loss is often encoded through the discrete probability transitions. For instance, a state s which deterministically transitions to a close state s' in \mathcal{M} such that $\phi_i(s) = \bar{s} = \phi_i(s')$ induces $\bar{\mathbf{P}}_{\bar{\pi}_\theta}(\bar{s} | \bar{s}) > 0$. Observe that the PAC computation of $\hat{L}_{\mathcal{P}}^{\xi_{\bar{\pi}_\theta}}$ is sensitive to the entropy of $\bar{\mathbf{P}}_\theta$, which thus may induce a residual transition loss. $L_{\mathcal{P}}^{\xi_{\bar{\pi}_\theta}}$ is on the contrary not sensitive to this. In practice, its value will thus often be lower than its approximated upper bound $\hat{L}_{\mathcal{P}}^{\xi_{\bar{\pi}_\theta}}$.

Policy distillation. The guarantees derived in Sect. 3 are only valid for $\bar{\pi}_\theta$, the policy under which formal properties can be verified. We further need evaluate if it achieves sound performance in the RL environment: checking the expected value difference via Thm. 3.5 is most significant

when $V_{\bar{\pi}_\theta}(s)$ is worth in any state s likely to be reached in $\mathcal{M}_{\bar{\pi}_\theta}$. We compare the episode return achieved by $\bar{\pi}_\theta$ against π in the environment \mathcal{M} (Fig. 2c). Our framework allows learning to improve $\bar{\pi}_\theta$ along training steps and eventually achieving the return of the original policy π . This illustrates that training our latent model enables distilling π into a latent policy $\bar{\pi}_\theta$ that achieves similar performance in \mathcal{M} .

6 Conclusion

In this work, we presented VAE-MDPs, a framework for learning discrete latent models of unknown, continuous-spaces environments with bisimulation guarantees. We detailed how such latent models can be learned by executing an RL policy in the environment and showed that the procedure yields a distilled version of the latter as a side effect. To provide the guarantees, we introduced new local losses bounds aimed at discrete latent spaces with their PAC-efficient approximation algorithm derived from the execution of the distilled policy. All this enables the verification of RL policies for unknown continuous MDPs.

Experimental results demonstrate the feasibility of our approach through the PAC bounds and the performance of the distilled policy achieved for various environments. Our tool can also be used to highlight the lack of robustness of input policies when the distillation fails.

Complementary to safe-RL approaches addressed via formal methods, we emphasize the ability of our tool to be coupled with such algorithms when no model of the environment is known a priori. The applicability of our method enables its use in future work for real-world case studies and more complex settings, such as multi-agent systems.

Acknowledgments

This research received funding from the Flemish Government (AI Research Program) and was supported by the DESCARTES iBOF project. G.A. Perez is also supported by the Belgian FWO “SAILor” project (G030020N).

References

Alamdari, P. A.; Avni, G.; Henzinger, T. A.; and Lukina, A. 2020. Formal Methods with a Touch of Magic. In *2020 Formal Methods in Computer Aided Design, FMCAD 2020, Haifa, Israel, September 21-24, 2020*, 138–147. IEEE.

Alemi, A. A.; Poole, B.; Fischer, I.; Dillon, J. V.; Saurous, R. A.; and Murphy, K. 2018. Fixing a Broken ELBO. In Dy, J. G.; and Krause, A., eds., *Proceedings of the 35th International Conference on Machine Learning, ICML 2018, Stockholmsmässan, Stockholm, Sweden, July 10-15, 2018*, volume 80 of *Proceedings of Machine Learning Research*, 159–168. PMLR.

Alshiekh, M.; Bloem, R.; Ehlers, R.; Könighofer, B.; Niekum, S.; and Topcu, U. 2018. Safe Reinforcement Learning via Shielding. In McIlraith, S. A.; and Weinberger, K. Q., eds., *Proceedings of the Thirty-Second AAAI Conference on Artificial Intelligence, (AAAI-18), the 30th innovative Applications of Artificial Intelligence (IAAI-18), and the 8th AAAI*

Symposium on Educational Advances in Artificial Intelligence (EAAI-18), New Orleans, Louisiana, USA, February 2-7, 2018, 2669–2678. AAAI Press.

Bacci, E.; and Parker, D. 2020. Probabilistic Guarantees for Safe Deep Reinforcement Learning. In Bertrand, N.; and Jansen, N., eds., *Formal Modeling and Analysis of Timed Systems - 18th International Conference, FORMATS 2020, Vienna, Austria, September 1-3, 2020, Proceedings*, volume 12288 of *LNCS*, 231–248. Springer.

Brockman, G.; Cheung, V.; Petteersson, L.; Schneider, J.; Schulman, J.; Tang, J.; and Zaremba, W. 2016. OpenAI Gym. *CoRR*, abs/1606.01540.

Budde, C. E.; Hartmanns, A.; Klauck, M.; Kretínský, J.; Parker, D.; Quatmann, T.; Turrini, A.; and Zhang, Z. 2020. On Correctness, Precision, and Performance in Quantitative Verification - QComp 2020 Competition Report. In Margaria, T.; and Steffen, B., eds., *Leveraging Applications of Formal Methods, Verification and Validation: Tools and Trends - 9th International Symposium on Leveraging Applications of Formal Methods, ISoLA 2020, Rhodes, Greece, October 20-30, 2020, Proceedings, Part IV*, volume 12479 of *LNCS*, 216–241. Springer.

Burden, J.; Siahroudi, S. K.; and Kudenko, D. 2021. Latent Property State Abstraction For Reinforcement learning. In *Proceedings of the AAMAS Workshop on Adaptive Learning Agents (ALA)*.

Burke, M.; Hristov, Y.; and Ramamoorthy, S. 2019. Hybrid system identification using switching density networks. In Kaelbling, L. P.; Kragic, D.; and Sugiura, K., eds., *3rd Annual Conference on Robot Learning, CoRL 2019, Osaka, Japan, October 30 - November 1, 2019, Proceedings*, volume 100 of *Proceedings of Machine Learning Research*, 172–181. PMLR.

Carr, S.; Jansen, N.; and Topcu, U. 2020. Verifiable RNN-Based Policies for POMDPs Under Temporal Logic Constraints. In Bessiere, C., ed., *Proceedings of the Twenty-Ninth International Joint Conference on Artificial Intelligence, IJCAI 2020*, 4121–4127. ijcai.org.

Chatterjee, K.; de Alfaro, L.; Majumdar, R.; and Raman, V. 2008. Algorithms for Game Metrics. In Hariharan, R.; Mukund, M.; and Vinay, V., eds., *IARCS Annual Conference on Foundations of Software Technology and Theoretical Computer Science, FSTTCS 2008, December 9-11, 2008, Bangalore, India*, volume 2 of *LIPICs*, 107–118. Schloss Dagstuhl - Leibniz-Zentrum für Informatik.

Chen, D.; van Breugel, F.; and Worrell, J. 2012. On the Complexity of Computing Probabilistic Bisimilarity. In Birkedal, L., ed., *Foundations of Software Science and Computational Structures - 15th International Conference, FOSSACS 2012, Tallinn, Estonia, March 24 - April 1, 2012. Proceedings*, volume 7213 of *LNCS*, 437–451. Springer.

Corneil, D. S.; Gerstner, W.; and Brea, J. 2018. Efficient ModelBased Deep Reinforcement Learning with Variational State Tabulation. In Dy, J. G.; and Krause, A., eds., *Proceedings of the 35th International Conference on Machine Learning, ICML 2018, Stockholmsmässan, Stockholm, Swe-*

- den, July 10-15, 2018, volume 80 of *Proceedings of Machine Learning Research*, 1057–1066. PMLR.
- Desharnais, J.; Gupta, V.; Jagadeesan, R.; and Panangaden, P. 2004. Metrics for labelled Markov processes. *Theor. Comput. Sci.*, 318(3): 323–354.
- Dong, Z.; Seybold, B. A.; Murphy, K.; and Bui, H. H. 2020. Collapsed Amortized Variational Inference for Switching Nonlinear Dynamical Systems. In *Proceedings of the 37th International Conference on Machine Learning, ICML 2020, 13-18 July 2020*, volume 119 of *Proceedings of Machine Learning Research*, 2638–2647. PMLR.
- Ferns, N.; Panangaden, P.; and Precup, D. 2005. Metrics for Markov Decision Processes with Infinite State Spaces. In *UAI '05, Proceedings of the 21st Conference in Uncertainty in Artificial Intelligence, Edinburgh, Scotland, July 26-29, 2005*, 201–208. AUAI Press.
- Ferns, N.; Precup, D.; and Knight, S. 2014. Bisimulation for Markov Decision Processes through Families of Functional Expressions. In van Breugel, F.; Kashefi, E.; Palamidessi, C.; and Rutten, J., eds., *Horizons of the Mind. A Tribute to Prakash Panangaden - Essays Dedicated to Prakash Panangaden on the Occasion of His 60th Birthday*, volume 8464 of *LNCS*, 319–342. Springer.
- Freeman, C. D.; Ha, D.; and Metz, L. 2019. Learning to Predict Without Looking Ahead: World Models Without Forward Prediction. In Wallach, H. M.; Larochelle, H.; Beygelzimer, A.; d'Alché-Buc, F.; Fox, E. B.; and Garnett, R., eds., *Advances in Neural Information Processing Systems 32: Annual Conference on Neural Information Processing Systems 2019, NeurIPS 2019, 8-14 December 2019, Vancouver, BC, Canada*, 5380–5391.
- Gelada, C.; Kumar, S.; Buckman, J.; Nachum, O.; and Belle-mare, M. G. 2019. DeepMDP: Learning Continuous Latent Space Models for Representation Learning. In Chaudhuri, K.; and Salakhutdinov, R., eds., *Proceedings of the 36th International Conference on Machine Learning, ICML 2019, 9-15 June 2019, Long Beach, California, USA*, volume 97 of *Proceedings of Machine Learning Research*, 2170–2179. PMLR.
- Genevay, A.; Chizat, L.; Bach, F. R.; Cuturi, M.; and Peyré, G. 2019. Sample Complexity of Sinkhorn Divergences. In Chaudhuri, K.; and Sugiyama, M., eds., *The 22nd International Conference on Artificial Intelligence and Statistics, AISTATS 2019, 16-18 April 2019, Naha, Okinawa, Japan*, volume 89 of *Proceedings of Machine Learning Research*, 1574–1583. PMLR.
- Givan, R.; Dean, T. L.; and Greig, M. 2003. Equivalence notions and model minimization in Markov decision processes. *Artif. Intell.*, 147(1-2): 163–223.
- Haarnoja, T.; Zhou, A.; Abbeel, P.; and Levine, S. 2018. Soft Actor-Critic: Off-Policy Maximum Entropy Deep Reinforcement Learning with a Stochastic Actor. In Dy, J. G.; and Krause, A., eds., *Proceedings of the 35th International Conference on Machine Learning, ICML 2018, Stockholmsmässan, Stockholm, Sweden, July 10-15, 2018*, volume 80 of *Proceedings of Machine Learning Research*, 1856–1865. PMLR.
- Hartmanns, A.; and Hermanns, H. 2014. The Modest Toolset: An Integrated Environment for Quantitative Modelling and Verification. In Ábrahám, E.; and Havelund, K., eds., *Tools and Algorithms for the Construction and Analysis of Systems - 20th International Conference, TACAS 2014, Grenoble, France, April 5-13, 2014. Proceedings*, volume 8413 of *LNCS*, 593–598. Springer.
- Hensel, C.; Junges, S.; Katoen, J.-P.; Quatmann, T.; and Volk, M. 2021. The probabilistic model checker Storm. *International Journal on Software Tools for Technology Transfer*.
- Hoeffding, W. 1963. Probability Inequalities for Sums of Bounded Random Variables. *Journal of the American Statistical Association*, 58(301): 13–30.
- Hoffman, M. D.; Blei, D. M.; Wang, C.; and Paisley, J. W. 2013. Stochastic variational inference. *J. Mach. Learn. Res.*, 14(1): 1303–1347.
- Huang, B. 2020. Steady State Analysis of Episodic Reinforcement Learning. In Larochelle, H.; Ranzato, M.; Hadsell, R.; Balcan, M.; and Lin, H., eds., *Advances in Neural Information Processing Systems 33: Annual Conference on Neural Information Processing Systems 2020, NeurIPS 2020, December 6-12, 2020, virtual*.
- Jang, E.; Gu, S.; and Poole, B. 2017. Categorical Reparameterization with Gumbel-Softmax. In *5th International Conference on Learning Representations, ICLR 2017, Toulon, France, April 24-26, 2017, Conference Track Proceedings*. OpenReview.net.
- Jansen, N.; Könighofer, B.; Junges, S.; Serban, A.; and Bloem, R. 2020. Safe Reinforcement Learning Using Probabilistic Shields (Invited Paper). In Konnov, I.; and Kovács, L., eds., *31st International Conference on Concurrency Theory (CONCUR 2020)*, volume 171 of *Leibniz International Proceedings in Informatics (LIPIcs)*, 3:1–3:16. Dagstuhl, Germany: Schloss Dagstuhl–Leibniz-Zentrum für Informatik. ISBN 978-3-95977-160-3.
- Junges, S.; Jansen, N.; Dehnert, C.; Topcu, U.; and Katoen, J. 2016. Safety-Constrained Reinforcement Learning for MDPs. In Chechik, M.; and Raskin, J., eds., *Tools and Algorithms for the Construction and Analysis of Systems - 22nd International Conference, TACAS 2016, Eindhoven, The Netherlands, April 2-8, 2016, Proceedings*, volume 9636 of *LNCS*, 130–146. Springer.
- Kearns, M. J.; Mansour, Y.; and Ng, A. Y. 2002. A Sparse Sampling Algorithm for Near-Optimal Planning in Large Markov Decision Processes. *Mach. Learn.*, 49(2-3): 193–208.
- Kingma, D. P.; and Welling, M. 2014. Auto-Encoding Variational Bayes. In Bengio, Y.; and LeCun, Y., eds., *2nd International Conference on Learning Representations, ICLR 2014, Banff, AB, Canada, April 14-16, 2014, Conference Track Proceedings*.
- Kwiatkowska, M.; Norman, G.; and Parker, D. 2011. PRISM 4.0: Verification of Probabilistic Real-time Systems. In Gopalakrishnan, G.; and Qadeer, S., eds., *Proc. 23rd International Conference on Computer Aided Verification (CAV'11)*, volume 6806 of *LNCS*, 585–591. Springer.

Larsen, K. G.; and Skou, A. 1989. Bisimulation Through Probabilistic Testing. In *Conference Record of the Sixteenth Annual ACM Symposium on Principles of Programming Languages, Austin, Texas, USA, January 11-13, 1989*, 344–352. ACM Press.

Lee, A. X.; Nagabandi, A.; Abbeel, P.; and Levine, S. 2020. Stochastic Latent Actor-Critic: Deep Reinforcement Learning with a Latent Variable Model. In Larochelle, H.; Ranzato, M.; Hadsell, R.; Balcan, M.; and Lin, H., eds., *Advances in Neural Information Processing Systems 33: Annual Conference on Neural Information Processing Systems 2020, NeurIPS 2020, December 6-12, 2020, virtual*.

Maddison, C. J.; Mnih, A.; and Teh, Y. W. 2017. The Concrete Distribution: A Continuous Relaxation of Discrete Random Variables. In *5th International Conference on Learning Representations, ICLR 2017, Toulon, France, April 24-26, 2017, Conference Track Proceedings*.

Mnih, V.; Kavukcuoglu, K.; Silver, D.; Rusu, A. A.; Veness, J.; Bellemare, M. G.; Graves, A.; Riedmiller, M. A.; Fidjeland, A.; Ostrovski, G.; Petersen, S.; Beattie, C.; Sadik, A.; Antonoglou, I.; King, H.; Kumaran, D.; Wierstra, D.; Legg, S.; and Hassabis, D. 2015. Human-level control through deep reinforcement learning. *Nat.*, 518(7540): 529–533.

Nowe, A. 1994. *Synthesis of “safe” fuzzy controllers based on reinforcement learning*. Ph.D. thesis, Vrije Universiteit Brussel.

Puterman, M. L. 1994. *Markov Decision Processes: Discrete Stochastic Dynamic Programming*. Wiley Series in Probability and Statistics. Wiley. ISBN 978-0-47161977-2.

Ren, T.; Niu, J.; Cui, J.; Ouyang, Z.; and Liu, X. 2021. An application of multi-objective reinforcement learning for efficient model-free control of canals deployed with IoT networks. *Journal of Network and Computer Applications*, 182: 103049.

Schaul, T.; Quan, J.; Antonoglou, I.; and Silver, D. 2016. Prioritized Experience Replay. In Bengio, Y.; and LeCun, Y., eds., *4th International Conference on Learning Representations, ICLR 2016, San Juan, Puerto Rico, May 2-4, 2016, Conference Track Proceedings*.

Simão, T. D.; Jansen, N.; and Spaan, M. T. J. 2021. AlwaysSafe: Reinforcement Learning without Safety Constraint Violations during Training. In Dignum, F.; Lomuscio, A.; Endriss, U.; and Nowé, A., eds., *AAMAS '21: 20th International Conference on Autonomous Agents and Multiagent Systems, Virtual Event, United Kingdom, May 3-7, 2021*, 1226–1235. ACM.

Tsitsiklis, J. N. 1994. Asynchronous Stochastic Approximation and Q-Learning. *Mach. Learn.*, 16(3): 185–202.

Tsitsiklis, J. N.; and Roy, B. V. 1997. An analysis of temporal-difference learning with function approximation. *IEEE Trans. Autom. Control.*, 42(5): 674–690.

van Breugel, F.; and Worrell, J. 2001. Towards Quantitative Verification of Probabilistic Transition Systems. In Orejas, F.; Spirakis, P. G.; and van Leeuwen, J., eds., *Automata, Languages and Programming, 28th International Colloquium, ICALP 2001, Crete, Greece, July 8-12, 2001, Proceedings*, volume 2076 of *LNCS*, 421–432. Springer.

A Details on Discrepancy Measures

Let $P, Q \in \mathcal{P}(\mathcal{X})$ be probability distributions over \mathcal{X} with density functions p and q .

Wasserstein. The Kantorovich-Rubinstein duality allows formulating the Wasserstein distance between P and Q as

$$W_d(P, Q) = \sup_{f \in \mathcal{F}_d} \left| \mathbb{E}_{x \sim P} f(x) - \mathbb{E}_{y \sim Q} f(y) \right|,$$

where \mathcal{F}_d is the set of 1-Lipschitz functions, i.e., $\mathcal{F}_d = \{f : |f(x) - f(y)| \leq d(x, y)\}$.

Total Variation. One can reformulate the total variation distance between P and Q as

$$\begin{aligned} d_{TV}(P, Q) &= \sup_{A \in \Sigma(\mathcal{X})} |P(A) - Q(A)| \\ &= \frac{1}{2} \int_{\mathcal{X}} |p(x) - q(x)| dx. \end{aligned}$$

When \mathcal{X} is continuous, TV might thus give an overly strong measure of the numerical differences across probability distributions to all measurable sets since the distance between two point masses dx, dy is 1 unless $x = y$ (Ferns, Panangaden, and Precup 2005).

B Latent Space Models

From now on, fix MDP $\mathcal{M} = \langle \mathcal{S}, \mathcal{A}, \mathbf{P}, \mathcal{R}, \ell, \mathbf{AP}, s_I \rangle$ with latent space model $\langle \overline{\mathcal{M}}, \phi, \psi \rangle$, $\overline{\mathcal{M}} = \langle \overline{\mathcal{S}}, \overline{\mathcal{A}}, \overline{\mathbf{P}}, \overline{\mathcal{R}}, \overline{\ell}, \mathbf{AP}, \overline{s}_I \rangle$. We write $\overline{V}_{\overline{\pi}}$ for the value function of a policy $\overline{\pi} \in \overline{\Pi}^{\text{ml}}$ in $\overline{\mathcal{M}}$.

B.1 DeepMDPs

In the following, we recall DeepMDPs notions (from Gelada et al. 2019) that are useful to prove bisimulation distance (Lem. B.1, Lem. B.2) and value difference bounds (Lem. B.3, Lem. B.4).

Smooth-valuations. A policy $\overline{\pi} \in \overline{\Pi}^{\text{ml}}$ is said to be $K_{\overline{V}}\text{-}(d_{TV}\text{-})\text{smooth-valued}$ if $\sup_{\overline{s} \in \overline{\mathcal{S}}} |\overline{V}_{\overline{\pi}}(\overline{s})| \leq K_{\overline{V}}$ and if for all $\overline{a} \in \overline{\mathcal{A}}$, $\sup_{\overline{s} \in \overline{\mathcal{S}}} |\overline{Q}_{\overline{\pi}}(\overline{s}, \overline{a})| \leq K_{\overline{V}}$. Observe that all policies $\overline{\pi} \in \overline{\Pi}^{\text{ml}}$ are $(|\overline{\mathcal{R}}_{\overline{\pi}}^*|/1-\gamma)$ -smooth-valued, where $|\overline{\mathcal{R}}_{\overline{\pi}}^*| = \sup_{\overline{s} \in \overline{\mathcal{S}}} |\overline{\mathcal{R}}_{\overline{\pi}}(\overline{s})|$.

Lipschitzness. A policy $\overline{\pi} \in \overline{\Pi}^{\text{ml}}$ is $K_{\overline{V}}\text{-Lipschitz-valued}$ if for all $\overline{s}_1, \overline{s}_2 \in \overline{\mathcal{S}}$, $|\overline{V}_{\overline{\pi}}(\overline{s}_1) - \overline{V}_{\overline{\pi}}(\overline{s}_2)| \leq K_{\overline{V}} d_{\overline{\mathcal{S}}}(\overline{s}_1, \overline{s}_2)$ and for all $\overline{a} \in \overline{\mathcal{A}}$, $|\overline{Q}_{\overline{\pi}}(\overline{s}_1, \overline{a}) - \overline{Q}_{\overline{\pi}}(\overline{s}_2, \overline{a})| \leq K_{\overline{V}} d_{\overline{\mathcal{S}}}(\overline{s}_1, \overline{s}_2)$. The MDP $\overline{\mathcal{M}}$ is $\langle K_{\overline{\mathcal{R}}}, K_{\overline{\mathbf{P}}} \rangle\text{-Lipschitz}$ if for all $\overline{s}_1, \overline{s}_2 \in \overline{\mathcal{S}}$,

$$\begin{aligned} |\overline{\mathcal{R}}_{\overline{\pi}}(\overline{s}_1) - \overline{\mathcal{R}}_{\overline{\pi}}(\overline{s}_2)| &\leq K_{\overline{\mathcal{R}}} d_{\overline{\mathcal{S}}}(\overline{s}_1, \overline{s}_2), \\ W_{d_{\overline{\mathcal{S}}}}(\overline{\mathbf{P}}_{\overline{\pi}}(\cdot | \overline{s}_1), \overline{\mathbf{P}}_{\overline{\pi}}(\cdot | \overline{s}_2)) &\leq K_{\overline{\mathbf{P}}} d_{\overline{\mathcal{S}}}(\overline{s}_1, \overline{s}_2). \end{aligned}$$

Moreover, all latent policies $\overline{\pi} \in \overline{\Pi}^{\text{ml}}$ with $K_{\overline{\mathbf{P}}} \leq \frac{1}{\gamma}$ are $(K_{\overline{\mathcal{R}}}/1-\gamma K_{\overline{\mathbf{P}}})\text{-Lipschitz-valued}$ (Gelada et al. 2019, Lem. 1). In the discrete setting, we replace the Wasserstein term by TV and we omit the $d_{\overline{\mathcal{S}}}$ terms.

B.2 Bounded Bisimulation Distance

Lemma B.1. *Let $\overline{\pi} \in \overline{\Pi}^{\text{ml}}$, assume $\overline{\mathcal{M}}$ is discrete and $\langle K_{\overline{\mathcal{R}}}, K_{\overline{\mathbf{P}}} \rangle\text{-Lipschitz}$. Then, given the induced stationary distribution $\xi_{\overline{\pi}}$ in \mathcal{M} ,*

$$\begin{aligned} \mathbb{E}_{s \sim \xi_{\overline{\pi}}} \tilde{d}_{\overline{\pi}}^{\mathcal{R}}(s, \phi(s)) &\leq L_{\overline{\mathcal{R}}}^{\xi_{\overline{\pi}}} + \gamma L_{\overline{\mathbf{P}}}^{\xi_{\overline{\pi}}} \frac{K_{\overline{\mathcal{R}}}^{\overline{\pi}}}{1 - \gamma K_{\overline{\mathbf{P}}}^{\overline{\pi}}}, \\ \mathbb{E}_{s \sim \xi_{\overline{\pi}}} \tilde{d}_{\overline{\pi}}^{\ell}(s, \phi(s)) &\leq \frac{\gamma L_{\overline{\mathbf{P}}}^{\xi_{\overline{\pi}}}}{1 - \gamma}. \end{aligned}$$

Proof. Gelada et al. (2019, Lemma A.4) showed that $\tilde{d}_{\overline{\pi}}^{\mathcal{R}}$ is $\frac{(1-\gamma)K_{\overline{\mathcal{R}}}^{\overline{\pi}}}{1-\gamma K_{\overline{\mathbf{P}}}^{\overline{\pi}}}$ -Lipschitz in $\overline{\mathcal{S}}$, whereas $\tilde{d}_{\overline{\pi}}^{\ell}$ is 1-Lipschitz since it assigns a maximal distance of one whenever states have different labels. Let $K_{\overline{\mathcal{R}}} = \frac{(1-\gamma)K_{\overline{\mathcal{R}}}^{\overline{\pi}}}{1-\gamma K_{\overline{\mathbf{P}}}^{\overline{\pi}}}$, $K_{\ell} = 1$ and $\varphi \in \{\mathcal{R}, \ell\}$, this allows us

deriving the following inequality:

$$\begin{aligned}
& \mathbb{E}_{s \sim \xi_{\bar{\pi}}} W_{\tilde{d}_{\bar{\pi}}^{\varphi}}(\phi \mathbf{P}_{\bar{\pi}}(\cdot | s), \bar{\mathbf{P}}_{\bar{\pi}}(\cdot | \phi(s))) \\
&= \mathbb{E}_{s \sim \xi_{\bar{\pi}}} \left[\inf_{\lambda \in \Lambda(\phi \mathbf{P}_{\bar{\pi}}(\cdot | s), \bar{\mathbf{P}}_{\bar{\pi}}(\cdot | \phi(s)))} \sum_{\bar{s}_1, \bar{s}_2 \in \bar{\mathcal{S}}} \tilde{d}_{\bar{\pi}}^{\varphi}(\bar{s}_1, \bar{s}_2) \lambda(\bar{s}_1, \bar{s}_2) \right] \\
&\leq \mathbb{E}_{s \sim \xi_{\bar{\pi}}} \left[\inf_{\lambda \in \Lambda(\phi \mathbf{P}_{\bar{\pi}}(\cdot | s), \bar{\mathbf{P}}_{\bar{\pi}}(\cdot | \phi(s)))} \sum_{\bar{s}_1, \bar{s}_2 \in \bar{\mathcal{S}}} K_{\varphi} \mathbf{1}_{\bar{s}_1 \neq \bar{s}_2} \lambda(\bar{s}_1, \bar{s}_2) \right] \quad (\tilde{d}_{\bar{\pi}}^{\varphi} \text{ is } K_{\varphi}\text{-Lipschitz in } \bar{\mathcal{S}}) \\
&= K_{\varphi} \mathbb{E}_{s \sim \xi_{\bar{\pi}}} \left[\inf_{\lambda \in \Lambda(\phi \mathbf{P}_{\bar{\pi}}(\cdot | s), \bar{\mathbf{P}}_{\bar{\pi}}(\cdot | \phi(s)))} \sum_{\bar{s}_1 \neq \bar{s}_2} \lambda(\bar{s}_1, \bar{s}_2) \right] \\
&= K_{\varphi} \mathbb{E}_{s \sim \xi_{\bar{\pi}}} d_{TV}(\phi \mathbf{P}_{\bar{\pi}}(\cdot | s), \bar{\mathbf{P}}_{\bar{\pi}}(\cdot | \phi(s))) \quad (\text{by definition of TV; TV coincides with } W_{\mathbf{1}_{\neq}}) \\
&= K_{\varphi} \mathbb{E}_{s \sim \xi_{\bar{\pi}}} \left[\frac{1}{2} \sum_{\bar{s}' \in \bar{\mathcal{S}}} |\phi \mathbf{P}_{\bar{\pi}}(\bar{s}' | s) - \bar{\mathbf{P}}_{\bar{\pi}}(\bar{s}' | \phi(s))| \right] \\
&= K_{\varphi} \mathbb{E}_{s \sim \xi_{\bar{\pi}}} \left[\frac{1}{2} \sum_{\bar{s}' \in \bar{\mathcal{S}}} \left| \mathbb{E}_{\bar{a} \sim \bar{\pi}(\cdot | s)} \phi \mathbf{P}(\bar{s}' | s, \bar{a}) - \mathbb{E}_{\bar{a} \sim \bar{\pi}(\cdot | \phi(s))} \bar{\mathbf{P}}(\bar{s}' | \phi(s), \bar{a}) \right| \right] \\
&= K_{\varphi} \mathbb{E}_{s \sim \xi_{\bar{\pi}}} \left[\frac{1}{2} \sum_{\bar{s}' \in \bar{\mathcal{S}}} \left| \mathbb{E}_{\bar{a} \sim \bar{\pi}(\cdot | s)} (\phi \mathbf{P}(\bar{s}' | s, \bar{a}) - \bar{\mathbf{P}}(\bar{s}' | \phi(s), \bar{a})) \right| \right] \\
&\leq K_{\varphi} \mathbb{E}_{s \sim \xi_{\bar{\pi}}} \mathbb{E}_{\bar{a} \sim \bar{\pi}(\cdot | s)} \left[\frac{1}{2} \sum_{\bar{s}' \in \bar{\mathcal{S}}} |\phi \mathbf{P}(\bar{s}' | s, \bar{a}) - \bar{\mathbf{P}}(\bar{s}' | \phi(s), \bar{a})| \right] \quad (\text{Jensen's inequality}) \\
&\leq K_{\varphi} L_{\mathbf{P}}^{\xi_{\bar{\pi}}}.
\end{aligned}$$

Then,

$$\begin{aligned}
& \mathbb{E}_{s \sim \xi_{\bar{\pi}}} \tilde{d}_{\bar{\pi}}^{\varphi}(s, \phi(s)) \\
&= \mathbb{E}_{s \sim \xi_{\bar{\pi}}} \left[(1 - \gamma) |\mathcal{R}_{\bar{\pi}}(s) - \bar{\mathcal{R}}_{\bar{\pi}}(\phi(s))| \cdot \mathbf{1}_{\{\mathcal{R}\}}(\varphi) + \gamma W_{\tilde{d}_{\bar{\pi}}^{\varphi}}(\mathbf{P}_{\bar{\pi}}(\cdot | s), \bar{\mathbf{P}}_{\bar{\pi}}(\cdot | \phi(s))) \right] \quad (\ell(s) = \ell(\phi(s)) \text{ by Assumption 3.3}) \\
&\leq (1 - \gamma) L_{\mathcal{R}}^{\xi_{\bar{\pi}}} \cdot \mathbf{1}_{\{\mathcal{R}\}}(\varphi) + \gamma \mathbb{E}_{s \sim \xi_{\bar{\pi}}} \left[W_{\tilde{d}_{\bar{\pi}}^{\varphi}}(\mathbf{P}_{\bar{\pi}}(\cdot | s), \bar{\mathbf{P}}_{\bar{\pi}}(\cdot | \phi(s))) \right] \\
&\leq (1 - \gamma) L_{\mathcal{R}}^{\xi_{\bar{\pi}}} \cdot \mathbf{1}_{\{\mathcal{R}\}}(\varphi) \\
&\quad + \gamma \mathbb{E}_{s \sim \xi_{\bar{\pi}}} \left[W_{\tilde{d}_{\bar{\pi}}^{\varphi}}(\mathbf{P}_{\bar{\pi}}(\cdot | s), \phi \mathbf{P}_{\bar{\pi}}(\cdot | s)) + W_{\tilde{d}_{\bar{\pi}}^{\varphi}}(\phi \mathbf{P}_{\bar{\pi}}(\cdot | s), \bar{\mathbf{P}}_{\bar{\pi}}(\cdot | \phi(s))) \right] \quad (\text{triangular inequality}) \\
&\leq (1 - \gamma) L_{\mathcal{R}}^{\xi_{\bar{\pi}}} \cdot \mathbf{1}_{\{\mathcal{R}\}}(\varphi) + \gamma K_{\varphi} L_{\mathbf{P}}^{\xi_{\bar{\pi}}} + \gamma \mathbb{E}_{s \sim \xi_{\bar{\pi}}} W_{\tilde{d}_{\bar{\pi}}^{\varphi}}(\mathbf{P}_{\bar{\pi}}(\cdot | s), \phi \mathbf{P}_{\bar{\pi}}(\cdot | s)) \quad (\text{by the inequality derived above}) \\
&\leq (1 - \gamma) L_{\mathcal{R}}^{\xi_{\bar{\pi}}} \cdot \mathbf{1}_{\{\mathcal{R}\}}(\varphi) + \gamma K_{\varphi} L_{\mathbf{P}}^{\xi_{\bar{\pi}}} + \gamma \mathbb{E}_{s \sim \xi_{\bar{\pi}}} \tilde{d}_{\bar{\pi}}^{\varphi}(s, \phi(s)).
\end{aligned}$$

To see how we pass from the penultimate to the last line, recall that

$$\mathbb{E}_{s \sim \xi_{\bar{\pi}}} W_{\tilde{d}_{\bar{\pi}}^{\varphi}}(\mathbf{P}_{\bar{\pi}}(\cdot | s), \phi \mathbf{P}_{\bar{\pi}}(\cdot | s)) = \mathbb{E}_{s \sim \xi_{\bar{\pi}}} \sup_{f \in \mathcal{F}_{\tilde{d}_{\bar{\pi}}^{\varphi}}} \left| \mathbb{E}_{s' \sim \mathbf{P}_{\bar{\pi}}(\cdot | s)} f(s') - \mathbb{E}_{s' \sim \phi \mathbf{P}_{\bar{\pi}}(\cdot | s)} f(s') \right|,$$

where

$$\mathcal{F}_{\tilde{d}_{\bar{\pi}}^{\varphi}} = \{ f : \mathcal{S} \uplus \bar{\mathcal{S}} \rightarrow \mathbb{R} : |f(s_1^*) - f(s_2^*)| \leq \tilde{d}_{\bar{\pi}}^{\varphi}(s_1^*, s_2^*) \}.$$

Then, we have

$$\begin{aligned}
& \mathbb{E}_{s \sim \xi_{\bar{\pi}}} \sup_{f \in \mathcal{F}_{\tilde{d}_{\bar{\pi}}^{\varphi}}} \left| \mathbb{E}_{s' \sim \mathbf{P}_{\bar{\pi}}(\cdot|s)} f(s') - \mathbb{E}_{\bar{s}' \sim \phi_{\mathbf{P}_{\bar{\pi}}(\cdot|s)}} f(\bar{s}') \right| \\
&= \mathbb{E}_{s \sim \xi_{\bar{\pi}}} \sup_{f \in \mathcal{F}_{\tilde{d}_{\bar{\pi}}^{\varphi}}} \left| \mathbb{E}_{s' \sim \mathbf{P}_{\bar{\pi}}(\cdot|s)} f(s') - \mathbb{E}_{s' \sim \mathbf{P}_{\bar{\pi}}(\cdot|s)} f(\phi(s')) \right| \\
&= \mathbb{E}_{s \sim \xi_{\bar{\pi}}} \sup_{f \in \mathcal{F}_{\tilde{d}_{\bar{\pi}}^{\varphi}}} \left| \mathbb{E}_{s' \sim \mathbf{P}_{\bar{\pi}}(\cdot|s)} (f(s') - f(\phi(s'))) \right| \\
&\leq \mathbb{E}_{s \sim \xi_{\bar{\pi}}} \mathbb{E}_{s' \sim \mathbf{P}_{\bar{\pi}}(\cdot|s)} \sup_{f \in \mathcal{F}_{\tilde{d}_{\bar{\pi}}^{\varphi}}} |f(s') - f(\phi(s'))| \\
&= \mathbb{E}_{s \sim \xi_{\bar{\pi}}} \sup_{f \in \mathcal{F}_{\tilde{d}_{\bar{\pi}}^{\varphi}}} |f(s) - f(\phi(s))| \quad (\text{by the stationary property}) \\
&\leq \mathbb{E}_{s \sim \xi_{\bar{\pi}}} \tilde{d}_{\bar{\pi}}^{\varphi}(s, \phi(s)). \quad (\text{since } f \in \mathcal{F}_{\tilde{d}_{\bar{\pi}}^{\varphi}})
\end{aligned}$$

This finally yields

$$\begin{aligned}
(1 - \gamma) \mathbb{E}_{s \sim \xi_{\bar{\pi}}} \tilde{d}_{\bar{\pi}}^{\varphi}(s, \phi(s)) &\leq (1 - \gamma) L_{\mathcal{R}}^{\xi_{\bar{\pi}}} \cdot \mathbf{1}_{\{\mathcal{R}\}}(\varphi) + \gamma L_{\mathbf{P}}^{\xi_{\bar{\pi}}} K_{\varphi} \\
&\equiv \mathbb{E}_{s \sim \xi_{\bar{\pi}}} \tilde{d}_{\bar{\pi}}^{\varphi}(s, \phi(s)) \leq L_{\mathcal{R}}^{\xi_{\bar{\pi}}} \cdot \mathbf{1}_{\{\mathcal{R}\}}(\varphi) + \gamma L_{\mathbf{P}}^{\xi_{\bar{\pi}}} \frac{K_{\varphi}}{1 - \gamma}.
\end{aligned}$$

□

B.3 Abstraction Quality as Bounded Bisimulation Distance

Lemma B.2. *Let $\bar{\pi} \in \bar{\Pi}^{\text{ml}}$, assume $\bar{\mathcal{M}}$ is discrete and $\langle K_{\mathcal{R}}^{\bar{\pi}}, K_{\mathbf{P}}^{\bar{\pi}} \rangle$ -Lipschitz. Let $\xi_{\bar{\pi}}$ be the stationary distribution of \mathcal{M} induced by $\bar{\pi}$. Then, for any pair of states $s_1, s_2 \in \mathcal{S}$ such that $\phi(s_1) = \phi(s_2)$,*

$$\begin{aligned}
\tilde{d}_{\bar{\pi}}^{\mathcal{R}}(s_1, s_2) &\leq \left[L_{\mathcal{R}}^{\xi_{\bar{\pi}}} + \frac{\gamma L_{\mathbf{P}}^{\xi_{\bar{\pi}}} K_{\mathcal{R}}^{\bar{\pi}}}{1 - \gamma K_{\mathbf{P}}^{\bar{\pi}}} \right] (\xi_{\bar{\pi}}^{-1}(s_1) + \xi_{\bar{\pi}}^{-1}(s_2)), \\
\tilde{d}_{\bar{\pi}}^{\ell}(s_1, s_2) &\leq \frac{\gamma L_{\mathbf{P}}^{\xi_{\bar{\pi}}}}{1 - \gamma} (\xi_{\bar{\pi}}^{-1}(s_1) + \xi_{\bar{\pi}}^{-1}(s_2)).
\end{aligned}$$

Proof. Let $K_{\mathcal{R}} = \frac{(1-\gamma)K_{\bar{\mathcal{R}}}}{1-\gamma K_{\bar{\mathcal{R}}}}$, $K_{\ell} = 1$, and $\varphi \in \{\mathcal{R}, \ell\}$. We use the fact that $\tilde{d}_{\bar{\pi}}^{\varphi}(s, \phi(s)) \leq \xi_{\bar{\pi}}^{-1}(s) \mathbb{E}_{s \sim \xi_{\bar{\pi}}} \tilde{d}_{\bar{\pi}}^{\varphi}(s, \phi(s))$ for all $s \in \mathcal{S}$. Then, we have

$$\begin{aligned}
& \tilde{d}_{\bar{\pi}}^{\varphi}(s_1, s_2) \\
&\leq \tilde{d}_{\bar{\pi}}^{\varphi}(s_1, \phi(s_1)) + \tilde{d}_{\bar{\pi}}^{\varphi}(\phi(s_1), \phi(s_2)) + \tilde{d}_{\bar{\pi}}^{\varphi}(\phi(s_2), s_2) \quad (\text{triangular inequality}) \\
&\leq \xi_{\bar{\pi}}^{-1}(s_1) \mathbb{E}_{s \sim \xi_{\bar{\pi}}} \tilde{d}_{\bar{\pi}}^{\varphi}(s, \phi(s)) + \xi_{\bar{\pi}}^{-1}(s_2) \mathbb{E}_{s \sim \xi_{\bar{\pi}}} \tilde{d}_{\bar{\pi}}^{\varphi}(s, \phi(s)) + \tilde{d}_{\bar{\pi}}^{\varphi}(\phi(s_1), \phi(s_2)) \\
&\leq (\xi_{\bar{\pi}}^{-1}(s_1) + \xi_{\bar{\pi}}^{-1}(s_2)) \left(L_{\mathcal{R}}^{\xi_{\bar{\pi}}} \cdot \mathbf{1}_{\{\mathcal{R}\}}(\varphi) + \gamma L_{\mathbf{P}}^{\xi_{\bar{\pi}}} \frac{K_{\varphi}}{1 - \gamma} \right) + \tilde{d}_{\bar{\pi}}^{\varphi}(\phi(s_1), \phi(s_2)) \quad (\text{Lemma B.1}) \\
&= (\xi_{\bar{\pi}}^{-1}(s_1) + \xi_{\bar{\pi}}^{-1}(s_2)) \left(L_{\mathcal{R}}^{\xi_{\bar{\pi}}} \cdot \mathbf{1}_{\{\mathcal{R}\}}(\varphi) + \gamma L_{\mathbf{P}}^{\xi_{\bar{\pi}}} \frac{K_{\varphi}}{1 - \gamma} \right). \quad (\phi(s_1) = \phi(s_2) \text{ by assumption})
\end{aligned}$$

□

B.4 Value Difference Bound

Lemma B.3. *Let $\bar{\pi} \in \bar{\Pi}^{\text{ml}}$ and assume $\bar{\mathcal{M}}$ is discrete and $\langle K_{\mathcal{R}}^{\bar{\pi}}, K_{\mathbf{P}}^{\bar{\pi}} \rangle$ -Lipschitz. Let $\mathbf{C}, \mathbf{T} \subseteq \mathbf{AP}$, $\varphi \in \{\mathbf{CU}, \mathbf{T}, \diamond \mathbf{T}\}$ and $K_{\bar{\mathcal{V}}} = \min(|\bar{\mathcal{R}}_{\bar{\pi}}^*|/1-\gamma, K_{\bar{\mathcal{R}}}^{\bar{\pi}}/1-\gamma K_{\bar{\mathcal{P}}}^{\bar{\pi}})$. Then, given the induced stationary distribution $\xi_{\bar{\pi}}$ in \mathcal{M} ,*

$$\begin{aligned}
\mathbb{E}_{s, \bar{a} \sim \xi_{\bar{\pi}}} |Q_{\bar{\pi}}(s, \bar{a}) - \bar{Q}_{\bar{\pi}}(\phi(s), \bar{a})| &\leq \frac{L_{\mathcal{R}}^{\xi_{\bar{\pi}}} + \gamma K_{\bar{\mathcal{V}}} L_{\mathbf{P}}^{\xi_{\bar{\pi}}}}{1 - \gamma}, \\
\mathbb{E}_{s, \bar{a} \sim \xi_{\bar{\pi}}} |Q_{\bar{\pi}}^{\varphi}(s, \bar{a}) - \bar{Q}_{\bar{\pi}}^{\varphi}(\phi(s), \bar{a})| &\leq \frac{\gamma L_{\mathbf{P}}^{\xi_{\bar{\pi}}}}{1 - \gamma}.
\end{aligned}$$

Proof. The first result for discounted return follows directly from (Gelada et al. 2019). The choice of $K_{\bar{\mathcal{V}}}$ is derived from the fact that $K_{\bar{\mathbf{P}}}^{\xi_{\bar{\pi}}} \leq \frac{1}{\gamma}$ since $\bar{\mathcal{M}}$ is discrete: d_{TV} is bounded by one as well as the diameter of $\bar{\mathcal{S}}$, equipped with the discrete metric. For the reachability cases, first observe that $Q_{\bar{\pi}}^{\varphi}(s, \cdot) = 1$ when $s \in \llbracket \mathbb{T} \rrbracket \subseteq \mathcal{S}$ and $\bar{Q}_{\bar{\pi}}^{\varphi}(\bar{s}, \cdot) = 1$ when $\bar{s} \in \llbracket \mathbb{T} \rrbracket \subseteq \bar{\mathcal{S}}$. Moreover, if $\varphi = \text{CUT}$, $Q_{\bar{\pi}}^{\varphi}(s, \cdot) = 0$ when $s \in \llbracket \neg\text{C} \rrbracket \subseteq \mathcal{S}$ and $\bar{Q}_{\bar{\pi}}^{\varphi}(\bar{s}, \cdot) = 0$ when $\bar{s} \in \llbracket \neg\text{C} \rrbracket \subseteq \bar{\mathcal{S}}$. By Assumption 3.3, $s \in \llbracket \neg\text{C} \rrbracket \cup \llbracket \mathbb{T} \rrbracket$ implies that the value difference is zero since the labels of each state and those of its latent abstraction are the same. Therefore, let \mathbb{I} be $\mathbf{1}_{\llbracket \text{C} \rrbracket \cap \llbracket \neg\text{T} \rrbracket}$ if $\varphi = \text{CUT}$ and $\mathbf{1}_{\llbracket \neg\text{T} \rrbracket}$ if $\varphi = \diamond\text{T}$,

$$\begin{aligned}
& \mathbb{E}_{s, \bar{a} \sim \xi_{\bar{\pi}}} \left| Q_{\bar{\pi}}^{\varphi}(s, \bar{a}) - \bar{Q}_{\bar{\pi}}^{\varphi}(\phi(s), \bar{a}) \right| \\
&= \mathbb{E}_{s, \bar{a} \sim \xi_{\bar{\pi}}} \left[\mathbb{I}(s) \left| \mathbb{E}_{s' \sim \mathbf{P}(\cdot | s, \bar{a})} [\gamma V_{\bar{\pi}}^{\varphi}(s')] - \mathbb{E}_{\bar{s}' \sim \bar{\mathbf{P}}(\cdot | \phi(s), \bar{a})} [\gamma \bar{V}_{\bar{\pi}}^{\varphi}(\bar{s}')] \right| \right] \\
&\leq \gamma \mathbb{E}_{s, \bar{a} \sim \xi_{\bar{\pi}}} \left| \mathbb{E}_{s' \sim \mathbf{P}(\cdot | s, \bar{a})} V_{\bar{\pi}}^{\varphi}(s') - \mathbb{E}_{\bar{s}' \sim \bar{\mathbf{P}}(\cdot | \phi(s), \bar{a})} \bar{V}_{\bar{\pi}}^{\varphi}(\bar{s}') \right| \\
&\leq \gamma \mathbb{E}_{s, \bar{a} \sim \xi_{\bar{\pi}}} \left| \mathbb{E}_{s' \sim \mathbf{P}(\cdot | s, \bar{a})} [V_{\bar{\pi}}^{\varphi}(s') - \bar{V}_{\bar{\pi}}^{\varphi}(\phi(s'))] + \mathbb{E}_{\substack{\bar{s}' \sim \bar{\mathbf{P}}(\cdot | \phi(s), \bar{a}) \\ s' \sim \mathbf{P}(\cdot | s, \bar{a})}} [\bar{V}_{\bar{\pi}}^{\varphi}(\phi(s')) - \bar{V}_{\bar{\pi}}^{\varphi}(\bar{s}')] \right| \\
&\leq \gamma \mathbb{E}_{s, \bar{a} \sim \xi_{\bar{\pi}}} \left| \mathbb{E}_{s' \sim \mathbf{P}(\cdot | s, \bar{a})} [V_{\bar{\pi}}^{\varphi}(s') - \bar{V}_{\bar{\pi}}^{\varphi}(\phi(s'))] \right| + \gamma \mathbb{E}_{s, \bar{a} \sim \xi_{\bar{\pi}}} \left| \mathbb{E}_{\substack{\bar{s}' \sim \bar{\mathbf{P}}(\cdot | \phi(s), \bar{a}) \\ s' \sim \mathbf{P}(\cdot | s, \bar{a})}} [\bar{V}_{\bar{\pi}}^{\varphi}(\phi(s')) - \bar{V}_{\bar{\pi}}^{\varphi}(\bar{s}')] \right| \quad (\text{triangular inequality}) \\
&\leq \gamma \mathbb{E}_{s, \bar{a} \sim \xi_{\bar{\pi}}} \left| \mathbb{E}_{s' \sim \mathbf{P}(\cdot | s, \bar{a})} [V_{\bar{\pi}}^{\varphi}(s') - \bar{V}_{\bar{\pi}}^{\varphi}(\phi(s'))] \right| \\
&\quad + \gamma \mathbb{E}_{s, \bar{a} \sim \xi_{\bar{\pi}}} \left| \mathbb{E}_{s' \sim \mathbf{P}(\cdot | s, \bar{a})} \bar{V}_{\bar{\pi}}^{\varphi}(\phi(s')) - \mathbb{E}_{\bar{s}' \sim \bar{\mathbf{P}}(\cdot | \phi(s), \bar{a})} \bar{V}_{\bar{\pi}}^{\varphi}(\bar{s}') \right| \\
&\leq \gamma \mathbb{E}_{s, \bar{a} \sim \xi_{\bar{\pi}}} \left| \mathbb{E}_{s' \sim \mathbf{P}(\cdot | s, \bar{a})} [V_{\bar{\pi}}^{\varphi}(s') - \bar{V}_{\bar{\pi}}^{\varphi}(\phi(s'))] \right| + \gamma \mathbb{E}_{s, \bar{a} \sim \xi_{\bar{\pi}}} W_{\mathbf{1}_{\neq}}(\phi\mathbf{P}(\cdot | s, \bar{a}), \bar{\mathbf{P}}(\cdot | \phi(s), \bar{a})) \\
&\hspace{15em} (\text{by definition of the Wasserstein dual}) \\
&\leq \gamma \mathbb{E}_{s, \bar{a} \sim \xi_{\bar{\pi}}} \left| \mathbb{E}_{s' \sim \mathbf{P}(\cdot | s, \bar{a})} [V_{\bar{\pi}}^{\varphi}(s') - \bar{V}_{\bar{\pi}}^{\varphi}(\phi(s'))] \right| + \gamma L_{\bar{\mathbf{P}}}^{\xi_{\bar{\pi}}} \\
&\leq \gamma \mathbb{E}_{s, \bar{a} \sim \xi_{\bar{\pi}}} \mathbb{E}_{s' \sim \mathbf{P}(\cdot | s, \bar{a})} |V_{\bar{\pi}}^{\varphi}(s') - \bar{V}_{\bar{\pi}}^{\varphi}(\phi(s'))| + \gamma L_{\bar{\mathbf{P}}}^{\xi_{\bar{\pi}}} \quad (\text{Jensen's inequality}) \\
&\leq \gamma \mathbb{E}_{s \sim \xi_{\bar{\pi}}} |V_{\bar{\pi}}^{\varphi}(s) - \bar{V}_{\bar{\pi}}^{\varphi}(\phi(s))| + \gamma L_{\bar{\mathbf{P}}}^{\xi_{\bar{\pi}}} \quad (\text{by the stationary property}) \\
&= \gamma \mathbb{E}_{s \sim \xi_{\bar{\pi}}} \left| \mathbb{E}_{\bar{a} \sim \bar{\pi}(\cdot | \phi(s))} [Q_{\bar{\pi}}^{\varphi}(s, \bar{a}) - \bar{Q}_{\bar{\pi}}^{\varphi}(\phi(s), \bar{a})] \right| + \gamma L_{\bar{\mathbf{P}}}^{\xi_{\bar{\pi}}} \\
&\leq \gamma \mathbb{E}_{s, \bar{a} \sim \xi_{\bar{\pi}}} |Q_{\bar{\pi}}^{\varphi}(s, \bar{a}) - \bar{Q}_{\bar{\pi}}^{\varphi}(\phi(s), \bar{a})| + \gamma L_{\bar{\mathbf{P}}}^{\xi_{\bar{\pi}}} \quad (\text{Jensen's inequality})
\end{aligned}$$

Therefore,

$$\begin{aligned}
(1 - \gamma) \mathbb{E}_{s, \bar{a} \sim \xi_{\bar{\pi}}} |Q_{\bar{\pi}}^{\varphi}(s, \bar{a}) - \bar{Q}_{\bar{\pi}}^{\varphi}(\phi(s), \bar{a})| &\leq \gamma L_{\bar{\mathbf{P}}}^{\xi_{\bar{\pi}}}, \text{ i.e.,} \\
\mathbb{E}_{s, \bar{a} \sim \xi_{\bar{\pi}}} |Q_{\bar{\pi}}^{\varphi}(s, \bar{a}) - \bar{Q}_{\bar{\pi}}^{\varphi}(\phi(s), \bar{a})| &\leq \frac{\gamma L_{\bar{\mathbf{P}}}^{\xi_{\bar{\pi}}}}{1 - \gamma}
\end{aligned}$$

□

B.5 Abstraction Quality as Value Difference Bound

Lemma B.4. *Let $\bar{\pi} \in \bar{\Pi}^{\text{ml}}$ and assume $\bar{\mathcal{M}}$ is discrete and $\langle K_{\bar{\mathcal{R}}}^{\bar{\pi}}, K_{\bar{\mathbf{P}}}^{\bar{\pi}} \rangle$ -Lipschitz. Let $\text{C}, \text{T} \subseteq \mathbf{AP}$, $\varphi \in \{\text{CUT}, \diamond\text{T}\}$, $K_{\bar{\mathcal{V}}} = \min(|\bar{\mathcal{R}}^*|/1-\gamma, K_{\bar{\mathcal{R}}}^{\bar{\pi}}/1-\gamma K_{\bar{\mathbf{P}}}^{\bar{\pi}})$, and $\xi_{\bar{\pi}}$ be the induced stationary distribution in \mathcal{M} . Then, for any pair of states $s_1, s_2 \in \mathcal{S}$ such*

that $\phi(s_1) = \phi(s_2)$,

$$|V_{\bar{\pi}}(s_1) - V_{\bar{\pi}}(s_2)| \leq \frac{L_{\mathcal{R}}^{\xi_{\bar{\pi}}} + \gamma K_{\bar{V}} L_{\mathbf{P}}^{\xi_{\bar{\pi}}}}{1 - \gamma} (\xi_{\bar{\pi}}^{-1}(s_1) + \xi_{\bar{\pi}}^{-1}(s_2)),$$

$$|V_{\bar{\pi}}^{\varphi}(s_1) - V_{\bar{\pi}}^{\varphi}(s_2)| \leq \frac{\gamma L_{\mathbf{P}}^{\xi_{\bar{\pi}}}}{1 - \gamma} (\xi_{\bar{\pi}}^{-1}(s_1) + \xi_{\bar{\pi}}^{-1}(s_2)).$$

Proof. The discounted return case follows directly from Gelada et al. (2019) and Lemma B.3. For the reachability cases, we similarly use the fact that $\left| V_{\bar{\pi}}^{\varphi}(s) - \bar{V}_{\bar{\pi}}^{\varphi}(\phi(s)) \right| \leq \xi_{\bar{\pi}}^{-1}(s) \mathbb{E}_{s \sim \xi_{\bar{\pi}}} \left| V_{\bar{\pi}}^{\varphi}(s) - \bar{V}_{\bar{\pi}}^{\varphi}(\phi(s)) \right|$, which gives us

$$\begin{aligned} & |V_{\bar{\pi}}^{\varphi}(s_1) - V_{\bar{\pi}}^{\varphi}(s_2)| \\ &= \left| V_{\bar{\pi}}^{\varphi}(s_1) - \bar{V}_{\bar{\pi}}^{\varphi}(\phi(s_1)) + \bar{V}_{\bar{\pi}}^{\varphi}(\phi(s_1)) - \bar{V}_{\bar{\pi}}^{\varphi}(\phi(s_2)) + \bar{V}_{\bar{\pi}}^{\varphi}(\phi(s_2)) - V_{\bar{\pi}}^{\varphi}(s_2) \right| \\ &\leq \left| V_{\bar{\pi}}^{\varphi}(s_1) - \bar{V}_{\bar{\pi}}^{\varphi}(\phi(s_1)) \right| + \left| \bar{V}_{\bar{\pi}}^{\varphi}(\phi(s_1)) - \bar{V}_{\bar{\pi}}^{\varphi}(\phi(s_2)) \right| + \left| \bar{V}_{\bar{\pi}}^{\varphi}(\phi(s_2)) - V_{\bar{\pi}}^{\varphi}(s_2) \right| \quad (\text{triangular inequality}) \\ &\leq \xi_{\bar{\pi}}^{-1}(s_1) \mathbb{E}_{s \sim \xi_{\bar{\pi}}} \left| V_{\bar{\pi}}^{\varphi}(s) - \bar{V}_{\bar{\pi}}^{\varphi}(\phi(s)) \right| + \left| \bar{V}_{\bar{\pi}}^{\varphi}(\phi(s_1)) - \bar{V}_{\bar{\pi}}^{\varphi}(\phi(s_2)) \right| \\ &\quad + \xi_{\bar{\pi}}^{-1}(s_2) \mathbb{E}_{s \sim \xi_{\bar{\pi}}} \left| \bar{V}_{\bar{\pi}}^{\varphi}(\phi(s_2)) - V_{\bar{\pi}}^{\varphi}(s_2) \right| \\ &= \xi_{\bar{\pi}}^{-1}(s_1) \mathbb{E}_{s \sim \xi_{\bar{\pi}}} \left| V_{\bar{\pi}}^{\varphi}(s) - \bar{V}_{\bar{\pi}}^{\varphi}(\phi(s)) \right| + \xi_{\bar{\pi}}^{-1}(s_2) \mathbb{E}_{s \sim \xi_{\bar{\pi}}} \left| V_{\bar{\pi}}^{\varphi}(s) - \bar{V}_{\bar{\pi}}^{\varphi}(\phi(s)) \right| \quad (\phi(s_1) = \phi(s_2) \text{ by assumption}) \\ &\leq \frac{\gamma L_{\mathbf{P}}^{\xi_{\bar{\pi}}}}{1 - \gamma} (\xi_{\bar{\pi}}^{-1}(s_1) + \xi_{\bar{\pi}}^{-1}(s_2)) \quad (\text{by Lemma B.3}) \end{aligned}$$

□

B.6 Transition-reward function

In general RL environments, it is quite common for rewards to be generated from a reward function defined over transitions rather than over state-action pairs., i.e., $\mathcal{R}: \mathcal{S} \times \mathcal{A} \times \mathcal{S}$. In that case, we have $\mathcal{R}(s, a) = \mathbb{E}_{s' \sim \mathbf{P}(\cdot | s, a)} \mathcal{R}(s, a, s')$. Taking transition-rewards into account, we set up an upper bound on $L_{\mathcal{R}}^{\xi_{\bar{\pi}}}$ that can be efficiently estimated from samples (using Lemma 3.4).

Lemma B.5. *Let $\xi_{\bar{\pi}}$ be a stationary distribution of \mathcal{M} under $\bar{\pi} \in \bar{\Pi}^{\text{ml}}$, then*

$$L_{\mathcal{R}}^{\xi_{\bar{\pi}}} \leq \mathbb{E}_{s, \bar{a}, s' \sim \xi_{\bar{\pi}}} \left| \mathcal{R}(s, \bar{a}, s') - \bar{\mathcal{R}}(\phi(s), \bar{a}) \right| = \dot{L}_{\mathcal{R}}^{\xi_{\bar{\pi}}}.$$

Proof. The upper bound $\dot{L}_{\mathcal{R}}^{\xi_{\bar{\pi}}}$ on the local reward loss is given as follows:

$$\begin{aligned} & \mathbb{E}_{s, \bar{a} \sim \xi_{\bar{\pi}}} \left| \mathcal{R}(s, \bar{a}) - \bar{\mathcal{R}}(\phi(s), \bar{a}) \right| \\ &= \mathbb{E}_{s, \bar{a} \sim \xi_{\bar{\pi}}} \left| \mathbb{E}_{s' \sim \mathbf{P}(\cdot | s, \bar{a})} \mathcal{R}(s, \bar{a}, s') - \bar{\mathcal{R}}(\phi(s), \bar{a}) \right| \\ &\leq \mathbb{E}_{s, \bar{a} \sim \xi_{\bar{\pi}}} \mathbb{E}_{s' \sim \mathbf{P}(\cdot | s, \bar{a})} \left| \mathcal{R}(s, \bar{a}, s') - \bar{\mathcal{R}}(\phi(s), \bar{a}) \right| \quad (\text{Jensen's inequality}) \\ &= \mathbb{E}_{s, \bar{a}, s' \sim \xi_{\bar{\pi}}} \left| \mathcal{R}(s, \bar{a}, s') - \bar{\mathcal{R}}(\phi(s), \bar{a}) \right| \end{aligned}$$

□

This ensures Lem. 3.4 and Thm. 3.5 to remain valid by approximating $\dot{L}_{\mathcal{R}}^{\xi_{\bar{\pi}}}$ instead of $L_{\mathcal{R}}^{\xi_{\bar{\pi}}}$.

B.7 Local Transition Loss Upper Bound

Recall that to deal with general MDPs, we study an upper bound on $L_{\mathbf{P}}^{\xi_{\bar{\pi}}}$ (namely, $\dot{L}_{\mathbf{P}}^{\xi_{\bar{\pi}}}$) that can be efficiently approximated from samples. We derive it in the following Lemma.

Lemma B.6. *Let $\xi_{\bar{\pi}}$ be a stationary distribution of \mathcal{M} under $\bar{\pi} \in \bar{\Pi}^{\text{ml}}$, then*

$$L_{\mathbf{P}}^{\xi_{\bar{\pi}}} \leq \mathbb{E}_{s, \bar{a}, s' \sim \xi_{\bar{\pi}}} W_{d_{\bar{S}}}(\phi(\cdot | s'), \bar{\mathbf{P}}(\cdot | \phi(s), \bar{a})) = \dot{L}_{\mathbf{P}}^{\xi_{\bar{\pi}}}$$

where we write $\xi_{\bar{\pi}}(s, \bar{a}, s') = \xi_{\bar{\pi}}(s, \bar{a}) \cdot \mathbf{P}(s' | s, \bar{a})$ and $\phi(\bar{s} | s) = \mathbf{1}_{=}(\phi(s), \bar{s})$.

Proof. The upper bound $\hat{L}_{\mathbf{P}}^{\xi_{\bar{\pi}}}$ on the local transition loss is obtained as follows.

$$\begin{aligned}
& \mathbb{E}_{s, \bar{a} \sim \xi_{\bar{\pi}}} \sup_{f \in \mathcal{F}_{d_{\bar{S}}}} \left| \mathbb{E}_{\bar{s}_1 \sim \phi(\cdot | s, \bar{a})} f(\bar{s}_1) - \mathbb{E}_{\bar{s}_2 \sim \bar{\mathbf{P}}(\cdot | \phi(s), \bar{a})} f(\bar{s}_2) \right| \\
&= \mathbb{E}_{s, \bar{a} \sim \xi_{\bar{\pi}}} \sup_{f \in \mathcal{F}_{d_{\bar{S}}}} \left| \mathbb{E}_{s' \sim \mathbf{P}(\cdot | s, \bar{a})} f(\phi(s')) - \mathbb{E}_{\bar{s}_2 \sim \bar{\mathbf{P}}(\cdot | \phi(s), \bar{a})} f(\bar{s}_2) \right| \\
&= \mathbb{E}_{s, \bar{a} \sim \xi_{\bar{\pi}}} \sup_{f \in \mathcal{F}_{d_{\bar{S}}}} \left| \mathbb{E}_{s' \sim \mathbf{P}(\cdot | s, \bar{a})} \left[f(\phi(s')) - \mathbb{E}_{\bar{s}_2 \sim \bar{\mathbf{P}}(\cdot | \phi(s), \bar{a})} f(\bar{s}_2) \right] \right| \\
&\leq \mathbb{E}_{s, \bar{a} \sim \xi_{\bar{\pi}}} \sup_{f \in \mathcal{F}_{d_{\bar{S}}}} \mathbb{E}_{s' \sim \mathbf{P}(\cdot | s, \bar{a})} \left| f(\phi(s')) - \mathbb{E}_{\bar{s}_2 \sim \bar{\mathbf{P}}(\cdot | \phi(s), \bar{a})} f(\bar{s}_2) \right| \quad (\text{Jensen's inequality}) \\
&\leq \mathbb{E}_{s, \bar{a} \sim \xi_{\bar{\pi}}} \mathbb{E}_{s' \sim \mathbf{P}(\cdot | s, \bar{a})} \sup_{f \in \mathcal{F}_{d_{\bar{S}}}} \left| f(\phi(s')) - \mathbb{E}_{\bar{s}_2 \sim \bar{\mathbf{P}}(\cdot | \phi(s), \bar{a})} f(\bar{s}_2) \right| \\
&= \mathbb{E}_{s, \bar{a}, s' \sim \xi_{\bar{\pi}}} \sup_{f \in \mathcal{F}_{d_{\bar{S}}}} \left| \mathbb{E}_{\bar{s}_1 \sim \phi(\cdot | s')} f(\bar{s}_1) - \mathbb{E}_{\bar{s}_2 \sim \bar{\mathbf{P}}(\cdot | \phi(s), \bar{a})} f(\bar{s}_2) \right| \\
&= \mathbb{E}_{s, \bar{a}, s' \sim \xi_{\bar{\pi}}} W_{d_{\bar{S}}}(\phi(\cdot | s'), \bar{\mathbf{P}}(\cdot | \phi(s), \bar{a}))
\end{aligned}$$

□

B.8 Proof of Lemma 3.4

Proof. Since \mathcal{M} is ergodic, the agent acts in the BSCC induced by $\bar{\pi}$ and each tuple $\langle s_t, a_t, r_t, s_{t+1} \rangle$ can be considered to be drawn independently from the stationary distribution $\xi_{\bar{\pi}}$ of the BSCC in the limit. The result follows then from the Hoeffding's bound (Hoeffding 1963):

- consider the sequence of independent random variables $X_{0:T-1}^{\mathcal{R}}$ such that

$$X_t^{\mathcal{R}} = |r_t - \bar{\mathcal{R}}(\phi(s_t), \bar{a}_t)| \in [0, 1],$$

then $\hat{L}_{\mathcal{R}}^{\xi_{\bar{\pi}}} = \frac{1}{T} \sum_{t=0}^{T-1} X_t^{\mathcal{R}}$ and $\Pr\left(|L_{\mathcal{R}}^* - \hat{L}_{\mathcal{R}}^{\xi_{\bar{\pi}}}| \geq \varepsilon\right) \leq \delta_{\mathcal{R}}$, with $\delta_{\mathcal{R}} = 2e^{-2T\varepsilon^2}$ and $L_{\mathcal{R}}^* = L_{\mathcal{R}}^{\xi_{\bar{\pi}}}$ if \mathcal{R} is defined over state-action pairs and $L_{\mathcal{R}}^* = \hat{L}_{\mathcal{R}}^{\xi_{\bar{\pi}}}$ if it is defined over transitions.

- consider the sequence of random variables $X_{0:T-1}^{\mathbf{P}}$ such that

$$X_t^{\mathbf{P}} = 1 - \bar{\mathbf{P}}(\phi(s_{t+1}) | \phi(s_t), \bar{a}_t) \in [0, 1],$$

The latent MDP $\bar{\mathcal{M}}$ being discrete, we have

$$\begin{aligned}
\hat{L}_{\mathbf{P}}^{\xi_{\bar{\pi}}} &= \mathbb{E}_{s, \bar{a}, s' \sim \xi_{\bar{\pi}}} d_{TV}(\phi(\cdot | s'), \bar{\mathbf{P}}(\cdot | \phi(s), \bar{a})) \\
&= \mathbb{E}_{s, \bar{a}, s' \sim \xi_{\bar{\pi}}} \left[\frac{1}{2} \sum_{\bar{s}' \in \mathcal{S}} |\phi(\bar{s}' | s') - \bar{\mathbf{P}}(\bar{s}' | \phi(s), \bar{a})| \right] \\
&= \mathbb{E}_{s, \bar{a}, s' \sim \xi_{\bar{\pi}}} \left[\frac{1}{2} \cdot \left((1 - \bar{\mathbf{P}}(\phi(s') | \phi(s), \bar{a})) + \sum_{\bar{s}' \in \mathcal{S} \setminus \{\phi(s')\}} |0 - \bar{\mathbf{P}}(\bar{s}' | \phi(s), \bar{a})| \right) \right] \\
&\quad \text{(because } \phi(\bar{s}' | s') = 1 \text{ if } \phi(s') = \bar{s}' \text{ and 0 otherwise.)} \\
&= \mathbb{E}_{s, \bar{a}, s' \sim \xi_{\bar{\pi}}} \left[\frac{1}{2} \cdot \left((1 - \bar{\mathbf{P}}(\phi(s') | \phi(s), \bar{a})) + \sum_{\bar{s}' \in \mathcal{S} \setminus \{\phi(s')\}} \bar{\mathbf{P}}(\bar{s}' | \phi(s), \bar{a}) \right) \right] \\
&= \mathbb{E}_{s, \bar{a}, s' \sim \xi_{\bar{\pi}}} \left[\frac{1}{2} \cdot 2 \cdot (1 - \bar{\mathbf{P}}(\phi(s') | \phi(s), \bar{a})) \right] \\
&= \mathbb{E}_{s, \bar{a}, s' \sim \xi_{\bar{\pi}}} [1 - \bar{\mathbf{P}}(\phi(s') | \phi(s), \bar{a})]
\end{aligned}$$

then $\hat{L}_{\mathbf{P}}^{\xi_{\bar{\pi}}} = \frac{1}{T} \sum_{t=0}^{T-1} X_t^{\mathbf{P}}$ and $\Pr\left(|\hat{L}_{\mathbf{P}}^{\xi_{\bar{\pi}}} - L_{\mathbf{P}}^{\xi_{\bar{\pi}}}| \geq \varepsilon\right) \leq \delta_{\mathbf{P}}$, with $\delta_{\mathbf{P}} = 2e^{-2T\varepsilon^2}$.

Therefore,

$$\begin{aligned}
& \Pr\left(\left|L_{\mathcal{R}}^* - \hat{L}_{\mathcal{R}}^{\xi_{\bar{\pi}}}\right| \geq \varepsilon \vee \left|\hat{L}_{\mathbf{P}}^{\xi_{\bar{\pi}}} - \hat{L}_{\mathbf{P}}^{\xi_{\bar{\pi}}}\right| \geq \varepsilon\right) \\
& \leq \delta_{\mathcal{R}} + \delta_{\mathbf{P}} \\
& = 2e^{-2T\varepsilon^2} + 2e^{-2T\varepsilon^2} \\
& = 4e^{-2T\varepsilon^2}.
\end{aligned}$$

We thus consider $\delta \geq 4e^{-2T\varepsilon^2}$, i.e., $\log\left(\frac{\delta}{4}\right) \geq -2T\varepsilon^2$ and $T \geq \frac{-\log\left(\frac{\delta}{4}\right)}{2\varepsilon^2}$, which yields

$$\Pr\left(\left|L_{\mathcal{R}}^* - \hat{L}_{\mathcal{R}}^{\xi_{\bar{\pi}}}\right| \leq \varepsilon \wedge \left|\hat{L}_{\mathbf{P}}^{\xi_{\bar{\pi}}} - \hat{L}_{\mathbf{P}}^{\xi_{\bar{\pi}}}\right| \leq \varepsilon\right) \geq 1 - \delta.$$

□

B.9 Proof of Theorem 3.5

Proof. Let $\varepsilon' \in]0, 1[$ and $T \geq \left\lceil \frac{-\log\left(\frac{\delta}{4}\right)}{2\varepsilon'^2} \right\rceil$, then by applying Lemma B.3 and Lemma 3.4, we have

$$\begin{aligned}
\mathbb{E}_{s, \bar{a} \sim \xi_{\bar{\pi}}} \left| Q_{\bar{\pi}}(s, \bar{a}) - \bar{Q}_{\bar{\pi}}(\phi(s), \bar{a}) \right| & \leq \frac{L_{\mathcal{R}}^{\xi_{\bar{\pi}}} + \gamma K_{\bar{V}} L_{\mathbf{P}}^{\xi_{\bar{\pi}}}}{1 - \gamma} \leq \frac{\left(\hat{L}_{\mathcal{R}}^{\xi_{\bar{\pi}}} + \varepsilon'\right) + \gamma K_{\bar{V}} \left(\hat{L}_{\mathbf{P}}^{\xi_{\bar{\pi}}} + \varepsilon'\right)}{1 - \gamma}, \text{ and} \\
\mathbb{E}_{s, \bar{a} \sim \xi_{\bar{\pi}}} \left| Q_{\bar{\pi}}^{\varphi}(s, \bar{a}) - \bar{Q}_{\bar{\pi}}^{\varphi}(\phi(s), \bar{a}) \right| & \leq \frac{\gamma L_{\mathbf{P}}^{\xi_{\bar{\pi}}}}{1 - \gamma} \leq \frac{\gamma \left(\hat{L}_{\mathbf{P}}^{\xi_{\bar{\pi}}} + \varepsilon'\right)}{1 - \gamma}
\end{aligned}$$

with probability at least $1 - \delta$. To offer an error of at most ε , we need

$$\begin{aligned}
& \frac{\varepsilon' + \gamma K_{\bar{V}} \varepsilon'}{1 - \gamma} \leq \varepsilon \\
\equiv & \varepsilon' + \gamma K_{\bar{V}} \varepsilon' \leq \varepsilon(1 - \gamma) \\
\equiv & \varepsilon'(1 + \gamma K_{\bar{V}}) \leq \varepsilon(1 - \gamma) \\
\equiv & \varepsilon' \leq \frac{\varepsilon(1 - \gamma)}{1 + \gamma K_{\bar{V}}}
\end{aligned}$$

which yields the result. □

C Details on Variational MDPs

ELBO. In this work, we focus on the case where D_{KL} is used as divergence measure. The goal is thus to optimize $\min_{\theta} D_{\text{KL}}(\mathcal{M}_{\pi} \parallel P_{\theta})$, i.e., maximizing the marginal log-likelihood of traces of the original MDP $\mathbb{E}_{\hat{\tau} \sim \mathcal{M}_{\pi}} [\log P_{\theta}(\hat{\tau})]$. Recall that

$$P_{\theta}(\hat{\tau}) = \int_{\text{Traj}_{\bar{\mathcal{M}}_{\theta}}} P_{\theta}(\hat{\tau} \mid z_{0:T}) d\bar{\mathbf{P}}_{\bar{\pi}_{\theta}}(z_{0:T}) \quad (6)$$

where $\hat{\tau} = \langle s_{0:T}, a_{0:T-1}, r_{0:T-1}, l_{0:T} \rangle$, $z \in \mathcal{Z}$ such that $\mathcal{Z} = \bar{\mathcal{S}}$ if $\bar{\mathcal{A}} = \mathcal{A}$ and $\mathcal{Z} = \bar{\mathcal{S}} \times \bar{\mathcal{A}}$ otherwise, $\bar{\mathbf{P}}_{\bar{\pi}_{\theta}}(\bar{s}_{0:T}) = \prod_{t=0}^{T-1} \bar{\mathbf{P}}_{\bar{\pi}_{\theta}}(\bar{s}_{t+1} \mid \bar{s}_t)$, and $\bar{\mathbf{P}}_{\bar{\pi}_{\theta}}(\bar{s}_{0:T}, \bar{a}_{0:T-1}) = \prod_{t=0}^{T-1} \bar{\pi}_{\theta}(\bar{a}_t \mid \bar{s}_t) \cdot \bar{\mathbf{P}}_{\bar{\pi}_{\theta}}(\bar{s}_{t+1} \mid \bar{s}_t, \bar{a}_t)$. The dependency of $\hat{\tau}$ on \mathcal{Z} in Eq. 6 is made explicit by the law of total probability.

Optimizing $\mathbb{E}_{\hat{\tau} \sim \mathcal{M}_{\pi}} [\log P_{\theta}(\hat{\tau})]$ through Eq. 6 is typically intractable (Kingma and Welling 2014). To overcome this, we use an encoder $Q_{\iota}(z_{0:T} \mid \hat{\tau})$ to approximate the intractable true posterior $P_{\theta}(z_{0:T} \mid \hat{\tau}) = P_{\theta}(\hat{\tau} \mid z_{0:T}) \cdot \bar{\mathbf{P}}_{\bar{\pi}_{\theta}}(z_{0:T})/P_{\theta}(\hat{\tau})$. Such an encoder can be learned through the following optimization:

$$\min_{\iota, \theta} \mathbb{E}_{\hat{\tau} \sim \mathcal{M}_{\pi}} D(Q_{\iota}(\cdot \mid \hat{\tau}), P_{\theta}(\cdot \mid \hat{\tau})), \quad (7)$$

where D denotes a discrepancy measure. If we let once again D be D_{KL} , one can set a *lower bound* on the log-likelihood of

produced traces, often referred to as *evidence lower bound* (ELBO, Hoffman et al. 2013) as follows:

$$\begin{aligned}
& D_{\text{KL}}(Q_\iota(\cdot | \hat{\tau}) \| P_\theta(\cdot | \hat{\tau})) \\
&= \mathbb{E}_{z_{0:T} \sim Q_\iota(\cdot | \hat{\tau})} [\log Q_\iota(z_{0:T} | \hat{\tau}) - P_\theta(z_{0:T} | \hat{\tau})] \\
&= \mathbb{E}_{z_{0:T} \sim Q_\iota(\cdot | \hat{\tau})} [\log Q_\iota(z_{0:T} | \hat{\tau}) - \log P_\theta(\hat{\tau} | z_{0:T}) - \log \bar{\mathbf{P}}_{\bar{\pi}_\theta}(z_{0:T})] + \log P_\theta(\hat{\tau}) \\
\iff & \log P_\theta(\hat{\tau}) - D_{\text{KL}}(Q_\iota(\cdot | \hat{\tau}) \| P_\theta(\cdot | \hat{\tau})) \\
&= \mathbb{E}_{z_{0:T} \sim Q_\iota(\cdot | \hat{\tau})} [\log P_\theta(\hat{\tau} | z_{0:T}) + \log \bar{\mathbf{P}}_{\bar{\pi}_\theta}(z_{0:T}) - \log Q_\iota(z_{0:T} | \hat{\tau})]
\end{aligned}$$

Behavioral model. We assume that the behavioral model P_θ allows recovering the latent MDP parameters (i.e., $\bar{\mathbf{P}}_\theta$, $\bar{\mathcal{R}}_\theta$, and \bar{l}_θ), by decomposing it into reward and label models, the distilled policy, as well as a generative model P_θ^G allowing the reconstruction of states and actions. Therefore, states, actions, rewards, and labels are independent given the latent sequence:

$$\begin{aligned}
& P_\theta(s_{0:T}, a_{0:T-1}, r_{0:T-1}, l_{0:T} | \bar{s}_{0:T}) \\
&= P_\theta^G(s_{0:T} | \bar{s}_{0:T}) \cdot P_\theta(a_{0:T-1}, r_{0:T-1} | \bar{s}_{0:T}) \cdot P_\theta^\ell(l_{0:T} | \bar{s}_{0:T}) \\
&= P_\theta^G(s_{0:T} | \bar{s}_{0:T}) \cdot \bar{\pi}_\theta(a_{0:T-1} | \bar{s}_{0:T}) \cdot P_\theta^\mathcal{R}(r_{0:T-1} | \bar{s}_{0:T}, a_{0:T-1}) \cdot P_\theta^\ell(l_{0:T} | \bar{s}_{0:T}), \\
&\quad (\text{by the chain rule, } P_\theta(a_{0:T-1}, r_{0:T-1} | \bar{s}_{0:T}) = \bar{\pi}_\theta(a_{0:T-1} | \bar{s}_{0:T}) \cdot P_\theta^\mathcal{R}(r_{0:T-1} | \bar{s}_{0:T}, a_{0:T-1}))
\end{aligned}$$

and

$$\begin{aligned}
& P_\theta(s_{0:T}, a_{0:T-1}, r_{0:T-1}, l_{0:T} | \bar{s}_{0:T}, \bar{a}_{0:T-1}) \\
&= P_\theta^G(s_{0:T} | \bar{s}_{0:T}) \cdot P_\theta^G(a_{0:T-1} | \bar{s}_{0:T}, \bar{a}_{0:T-1}) \cdot P_\theta^\mathcal{R}(r_{0:T-1} | \bar{s}_{0:T}, \bar{a}_{0:T-1}) \cdot P_\theta^\ell(l_{0:T} | \bar{s}_{0:T})
\end{aligned}$$

Local setting. We formulate the ELBO in the local setting thanks to the following Lemma.

Lemma C.1. Let ξ_π be the stationary distribution of \mathcal{M}_π and $f: \mathcal{S} \times \mathcal{A} \times \text{Im}(\mathcal{R}) \times \mathcal{S} \rightarrow \mathbb{R}$ be a continuous function. Assume \mathcal{S}, \mathcal{A} are compact, then

$$\lim_{T \rightarrow \infty} \frac{1}{T} \mathbb{E}_{\hat{\tau} \sim \mathcal{M}_\pi[T]} \left[\sum_{t=0}^{T-1} f(s_t, a_t, r_t, s_{t+1}) \right] = \mathbb{E}_{s, a, r, s' \sim \xi_\pi} f(s, a, r, s')$$

where $\text{Traces}_{\mathcal{M}_\pi}(T)$ denotes the set of traces in \mathcal{M}_π of size T , $\mathcal{M}_\pi[T]$ denotes the distribution over $\text{Traces}_{\mathcal{M}_\pi}(T)$, and $\xi_\pi(s, a, r, s') = \xi_\pi(s, a, s') \cdot \mathbf{1}=(r, \mathcal{R}(s, a, s'))$.

Proof. First, observe that

$$\begin{aligned}
& \mathbb{E}_{\hat{\tau} \sim \mathcal{M}_\pi[T]} \left[\sum_{t=0}^{T-1} f(s_t, a_t, r_t, s_{t+1}) \right] \\
&= \mathbb{E}_{a_0 \sim \pi(\cdot | s_I)} \mathbb{E}_{s_1 \sim \mathbf{P}(\cdot | s_I, a_0)} \mathbb{E}_{a_1 \sim \pi(\cdot | s_1)} \cdots \mathbb{E}_{s_T \sim \mathbf{P}(\cdot | s_{T-1}, a_{T-1})} \left[\sum_{t=0}^{T-1} f(s_t, a_t, \mathcal{R}(s_t, a_t, s_{t+1}), s_{t+1}) \right] \\
&= \sum_{t=0}^{T-1} \mathbb{E}_{a_0 \sim \pi(\cdot | s_I)} \mathbb{E}_{s_1 \sim \mathbf{P}(\cdot | s_I, a_0)} \mathbb{E}_{a_1 \sim \pi(\cdot | s_1)} \cdots \mathbb{E}_{s_T \sim \mathbf{P}(\cdot | s_{T-1}, a_{T-1})} f(s_t, a_t, \mathcal{R}(s_t, a_t, s_{t+1}), s_{t+1}) \\
&= \sum_{t=0}^{T-1} \mathbb{E}_{\hat{\tau} \sim \mathcal{M}_\pi[t+1]} f(s_t, a_t, r_t, s_{t+1}).
\end{aligned}$$

Second, let $t \in \mathbb{N}$, $s, s' \in \mathcal{S}$, $a \in \text{Act}(s)$, and $r = \mathcal{R}(s, a, s')$, also observe that

$$\begin{aligned}
& \xi_\pi^t(s | s_I) = \int_{\text{Traces}_{\mathcal{M}_\pi}(t)} \mathbf{1}=(s_t, s) d\mathbb{P}_\pi(\text{Cyl}(s_{0:t}, a_{0:t-1})) \\
&\quad (\text{where } \text{Cyl}(s_{0:t}, a_{0:t}) = \{ \langle s_{0:\infty}^*, a_{0:\infty}^* \rangle \in \text{Traj}_{\mathcal{M}_\pi} \mid s_{i+1}^* = s_{i+1}, a_i^* = a_i \forall i \leq t-1 \}) \\
& f(s, a, r, s') \cdot \xi_\pi^t(s | s_I) = f(s, a, r, s') \cdot \int_{\text{Traces}_{\mathcal{M}_\pi}(t)} \mathbf{1}=(s_t, s) d\mathbb{P}_\pi(\text{Cyl}(s_{0:t}, a_{0:t-1})) \\
& \int_{\mathcal{S}} f(s, a, r, s') d\xi_\pi^t(s | s_I) = \int_{\mathcal{S}} \int_{\text{Traces}_{\mathcal{M}_\pi}(t)} f(s, a, r, s') \cdot \mathbf{1}=(s_t, s) d\mathbb{P}_\pi(\text{Cyl}(s_{0:t}, a_{0:t-1})) ds \\
&= \int_{\text{Traces}_{\mathcal{M}_\pi}(t)} f(s_t, a, r, s') d\mathbb{P}_\pi(\text{Cyl}(s_{0:t}, a_{0:t-1})).
\end{aligned}$$

Therefore, we have

$$\begin{aligned}
& \lim_{T \rightarrow \infty} \frac{1}{T} \mathbb{E}_{\hat{\tau} \sim \mathcal{M}_\pi[T]} \left[\sum_{t=0}^{T-1} f(s_t, a_t, r_t, s_{t+1}) \right] \\
&= \lim_{T \rightarrow \infty} \frac{1}{T} \sum_{t=0}^{T-1} \mathbb{E}_{\hat{\tau} \sim \mathcal{M}_\pi[t+1]} f(s_t, a_t, r_t, s_{t+1}) \\
&= \lim_{T \rightarrow \infty} \frac{1}{T} \sum_{t=0}^{T-1} \int_{\text{Traces}_{\mathcal{M}_\pi}(t+1)} f(s_t, a_t, r_t, s_{t+1}) d\mathbb{P}_\pi(\text{Cyl}(s_{0:t+1}, a_{0:t})) \\
&= \lim_{T \rightarrow \infty} \frac{1}{T} \sum_{t=0}^{T-1} \int_{\mathcal{S}} \int_{\mathcal{A}} \int_{\mathcal{S}} f(s, a, \mathcal{R}(s, a, s'), s') d\xi_\pi^t(s | s_I) d\pi(a | s) d\mathbf{P}(s' | s, a) \\
&= \lim_{T \rightarrow \infty} \int_{\mathcal{S}} \frac{1}{T} \sum_{t=0}^{T-1} \xi_\pi^t(ds | s_I) \int_{\mathcal{A}} \int_{\mathcal{S}} f(s, a, \mathcal{R}(s, a, s'), s') d\pi(a | s) d\mathbf{P}(s' | s, a).
\end{aligned}$$

By definition of ξ_π and Assumption 3.1, $\xi_\pi(A) = \lim_{T \rightarrow \infty} \frac{1}{T} \sum_{t=0}^{T-1} \xi_\pi^t(A | s)$ for all $s \in \mathcal{S}$, $A \in \Sigma(\mathcal{S})$, i.e., $\frac{1}{T} \sum_{t=0}^{T-1} \xi_\pi^t(A | s)$ weakly converges to ξ_π (e.g., Baier and Katoen 2008). By Assumption 3.2, the set of images of \mathcal{R} is a compact space. Therefore, f has compact support and by the Portmanteau's Theorem,

$$\begin{aligned}
& \lim_{T \rightarrow \infty} \int_{\mathcal{S}} \frac{1}{T} \sum_{t=0}^{T-1} \xi_\pi^t(ds | s_I) \int_{\mathcal{A}} \int_{\mathcal{S}} f(s, a, \mathcal{R}(s, a, s'), s') d\pi(a | s) d\mathbf{P}(s' | s, a) \\
&= \int_{\mathcal{S}} \xi_\pi(ds) \int_{\mathcal{A}} \int_{\mathcal{S}} f(s, a, \mathcal{R}(s, a, s'), s') d\pi(a | s) d\mathbf{P}(s' | s, a) \\
&= \mathbb{E}_{s, a, r, s' \sim \xi_\pi} f(s, a, r, s').
\end{aligned}$$

□

Corollary C.1.1. Let $\phi(\bar{s}, \bar{s}' | s, s') = \phi(\bar{s} | s)\phi(\bar{s}' | s')$, then

$$\begin{aligned}
& \lim_{T \rightarrow \infty} \frac{1}{T} \mathbb{E}_{\substack{\hat{\tau} \sim \mathcal{M}_\pi[T] \\ z_{0:T} \sim Q_\iota(\cdot | \hat{\tau})}} [\log P_\theta(\hat{\tau} | z_{0:T}) - D_{\text{KL}}(Q_\iota(\cdot | \hat{\tau}) \| P_\theta(\cdot | \hat{\tau}))] \\
&= \begin{cases} \mathbb{E}_{\substack{s, a, r, s' \sim \xi_\pi \\ \bar{s}, \bar{s}' \sim \phi_\iota(\cdot | s, s')}} [\log P_\theta^{\mathcal{G}}(s' | \bar{s}') + \log \bar{\pi}_\theta(a | \bar{s}) + \log P_\theta^{\mathcal{R}}(r | \bar{s}, a) \\ \quad - D_{\text{KL}}(\phi_\iota(\cdot | s') \| \bar{\mathbf{P}}_{\bar{\pi}_\theta}(\cdot | \bar{s}))] & \text{if } \bar{\mathcal{A}} = \mathcal{A}, \text{ and} \\ \mathbb{E}_{\substack{s, a, r, s' \sim \xi_\pi \\ \bar{s}, \bar{s}' \sim \phi_\iota(\cdot | s, s') \\ \bar{a} \sim Q_\iota^{\mathcal{A}}(\cdot | \bar{s}, a)}} [\log P_\theta^{\mathcal{G}}(s' | \bar{s}') + \log \psi_\theta(a | \bar{s}, \bar{a}) + \log P_\theta^{\mathcal{R}}(r | \bar{s}, \bar{a}) \\ \quad - D_{\text{KL}}(\phi_\iota(\cdot | s') \| \bar{\mathbf{P}}_\theta(\cdot | \bar{s})) \\ \quad - D_{\text{KL}}(Q_\iota^{\mathcal{A}}(\cdot | \bar{s}, a) \| \bar{\pi}_\theta(\cdot | \bar{s}))] & \text{otherwise,} \end{cases}
\end{aligned}$$

where $\hat{\tau} = \langle s_{0:T}, a_{0:T-1}, r_{0:T-1}, l_{0:T} \rangle$, $z_{0:T} = \bar{s}_{0:T}$ if $\bar{\mathcal{A}} = \mathcal{A}$ and $z_{0:T} = \langle \bar{s}_{0:T}, \bar{a}_{0:T-1} \rangle$ otherwise.

Proof. Taking

$$f(s, a, r, s') = \mathbb{E}_{\bar{s}, \bar{s}' \sim \phi_\iota(\cdot | s, s')} [g(\langle s, a, r, s' \rangle, \langle \bar{s}, \bar{s}' \rangle)]$$

with

$$\begin{aligned}
& g(\langle s, a, r, s' \rangle, \langle \bar{s}, \bar{s}' \rangle) \\
&= \begin{cases} \log(P_\theta^{\mathcal{G}}(s' | \bar{s}') \cdot P_\theta^{\mathcal{R}}(r | \bar{s}, a) \cdot \bar{\pi}_\theta(a | \bar{s})) - D_{\text{KL}}(\phi_\iota(\cdot | s') \| \bar{\mathbf{P}}_{\bar{\pi}_\theta}(\cdot | \bar{s})) & \text{if } \bar{\mathcal{A}} = \mathcal{A}, \text{ and} \\ \mathbb{E}_{\bar{a} \sim Q_\iota^{\mathcal{A}}(\cdot | \bar{s}, a)} \left[\log(P_\theta^{\mathcal{G}}(s' | \bar{s}') \cdot \psi_\theta(a | \bar{s}, \bar{a}) \cdot P_\theta^{\mathcal{R}}(r | \bar{s}, \bar{a})) \right. \\ \quad \left. - D_{\text{KL}}(\phi_\iota(\cdot | s') \| \bar{\mathbf{P}}_\theta(\cdot | \bar{s}, \bar{a})) \right] - D_{\text{KL}}(Q_\iota^{\mathcal{A}}(\cdot | \bar{s}, a) \| \bar{\pi}_\theta(\cdot | \bar{s})) & \text{otherwise} \end{cases}
\end{aligned}$$

yields the result. □

C.1 Latent Distributions

Discrete latent state space. W.l.o.g., we assume latent states to have a binary representation, we further see each bit as a Bernoulli random variable. Let $\alpha \in \mathbb{R}$ and $\lambda \in]0, 1]$, $\bar{s}_\lambda \in [0, 1]$ has a *relaxed Bernoulli distribution* $\bar{s}_\lambda \sim \text{RelaxedBernoulli}(\alpha, \lambda)$ with logit α and temperature parameter λ iff (a) if l is a logistic sample with location parameter $\alpha\lambda^{-1}$ and scale parameter λ^{-1} , i.e., $l \sim \text{Logistic}(\alpha\lambda^{-1}, \lambda^{-1})$, then $\bar{s}_\lambda = \sigma(l)$, σ being the *sigmoid* function, (b) $\lim_{\lambda \rightarrow 0} \text{RelaxedBernoulli}(\alpha, \lambda) = \text{Bernoulli}(\alpha)$, meaning $\mathbb{P}(\lim_{\lambda \rightarrow 0} \bar{s}_\lambda = 1) = \sigma(\alpha)$, and (c) let $p_{\alpha, \lambda}$ be the density of $\text{RelaxedBernoulli}(\alpha, \lambda)$, then $p_{\alpha, \lambda}(\bar{s}_\lambda)$ is log-convex in \bar{s}_λ . Since the logistic distribution belongs to the location-scale family, it is fully reparameterizable, i.e., $l \sim \text{Logistic}(\alpha\lambda^{-1}, \lambda^{-1}) \equiv x \sim \text{Logistic}(0, 1)$ and $l = \frac{\alpha + x}{\lambda}$. In practice, we train ϕ_ι and $\bar{\mathbf{P}}_\theta$ to infer and generate $\log_2 |\bar{\mathcal{S}}|$ logits, and we anneal λ to 0 during training while using Bernoulli distributions for evaluation. As suggested by Maddison, Mnih, and Teh (2017), we use two different temperature parameters and we fix their initial values to $\lambda_{\phi_\iota} = 2/3$ for the encoder distribution and $\lambda_{\mathbf{P}_\theta} = 1/2$ for the latent transition function.

Discrete latent action space. We learn discrete latent distributions for Q_ι^A and $\bar{\pi}_\theta$ by learning the logits of continuous relaxation of discrete distributions, through the *Gumbel softmax trick*. Let $n = |\bar{\mathcal{A}}|$, and $\bar{\mathcal{A}} = \{\bar{a}_1, \dots, \bar{a}_n\}$. Drawing $\bar{a}_i \sim \text{Categorical}(\boldsymbol{\alpha})$ from a discrete (categorical) distribution in $\mathcal{P}(\bar{\mathcal{A}})$ with logits parameter $\boldsymbol{\alpha} \in \mathbb{R}^n$ is equivalent to applying an arg max operator to the sum of *Gumbel samples* and these logits, i.e., $i = \arg \max_k [\boldsymbol{\alpha}_k - \log(-\log \epsilon_k)]$, where $\epsilon \in [0, 1]^n$ is a uniform noise. The sampling operator being fully reparameterizable here, arg max is however not derivable, preventing the operation to be optimized through gradient descent. The proposed solution is to replace the arg max operator by a softmax function with temperature parameter $\lambda \in]0, (n-1)^{-1}]$.

Concretely, $\mathbf{x} \in [0, 1]^n$ has a *relaxed discrete distribution* $\mathbf{x} \sim \text{RelaxedCategorical}(\boldsymbol{\alpha}, \lambda)$ with logits $\boldsymbol{\alpha}$, temperature parameter λ iff (a) let $\epsilon \in [0, 1]^n$ be a uniform noise and $\mathbf{G}_k = -\log(-\log \epsilon_k)$, then $\mathbf{x}_k = \frac{\exp((\boldsymbol{\alpha}_k + \mathbf{G}_k)\lambda^{-1})}{\sum_{i=1}^n \exp((\boldsymbol{\alpha}_i + \mathbf{G}_i)\lambda^{-1})}$ for each $k \in [n]$, (b) $\lim_{\lambda \rightarrow 0} \text{RelaxedCategorical}(\boldsymbol{\alpha}, \lambda) = \text{Categorical}(\boldsymbol{\alpha})$, meaning $\mathbb{P}(\lim_{\lambda \rightarrow 0} \mathbf{x}_k = 1) = \frac{\exp \boldsymbol{\alpha}_k}{\sum_{i=1}^n \exp \boldsymbol{\alpha}_i}$, and (c) let $p_{\boldsymbol{\alpha}, \lambda}$ be the density of $\text{RelaxedCategorical}(\boldsymbol{\alpha}, \lambda)$, then $p_{\boldsymbol{\alpha}, \lambda}(\mathbf{x})$ is log-convex in \mathbf{x} . In practice, we train Q_ι^A and $\bar{\pi}_\theta$ to infer and generate logits parameter $\boldsymbol{\alpha}$, and we anneal λ from $(n-1)^{-1}$ to 0 during training while using discrete distributions for evaluation. Again, as prescribed by Maddison, Mnih, and Teh (2017), we use two different temperature parameters, one for Q_ι^A and another one for $\bar{\pi}_\theta$.

C.2 Prioritized Experience Replay

Modern RL techniques allow to learn the parameters θ of a policy, model, or value function, by processing encountered experiences η via a loss function $L(\eta, \theta)$. If these are processed sequentially and discarded after all parameter updates, the latter are strongly correlated and rare events are quickly forgotten. *Prioritized experience replay buffers* (Schaul et al. 2016) are finite data structures \mathcal{D} that allow to overcome both issues by (i) storing experiences η with some assigned priority p_η , and (ii) producing $\eta \sim \mathcal{D}$ according to $P(\eta) = p_\eta^\zeta / \sum_{\eta' \in \mathcal{D}} p_{\eta'}^\zeta$, $\zeta \in [0, 1]$, which allows minimizing $\mathbb{E}_{\eta \sim \mathcal{D}} [w_\eta \cdot L(\eta, \theta)]$ for *importance sampling weight* $w_\eta > 0$. The replay buffer \mathcal{D} is *uniform* if $\zeta = 0$. Otherwise, when $\zeta > 0$, a bias is introduced because priorities change the real distribution of experiences and consequently the estimates of the expectation of L . This bias is alleviated via $w_\eta = (|\mathcal{D}| \cdot P(\eta))^{-\omega}$ for each $\eta \in \mathcal{D}$, $\omega \in [0, 1]$, where $\omega = 1$ fully corrects it.

We use prioritized replay buffers to store transitions and sample them when optimizing our loss function, i.e., ELBO. This allows to alleviate the posterior collapse problem, as shown in Figure 3. We introduced two priority functions, yielding a bucket-based and a loss-based prioritized replay buffer. In the following, we elaborate how precisely we assign priorities via the loss-based priority function.

Loss-based priorities. Draw $\langle s, a, r, s' \rangle \sim \xi_\pi$, we aim at assigning $p_{\langle s, a, r, s' \rangle}$ to its *individual transition loss*, i.e., L_{ELBO} : for $\bar{s}, \bar{s}' \sim \phi_\iota(\cdot | s, s')$, $\bar{a} \sim Q_\iota^A(\cdot | \bar{s}, a)$ if $\bar{\mathcal{A}} \neq \mathcal{A}$ and $\bar{a} = a$ else,

$$\begin{aligned} & L_{\text{ELBO}}(\langle s, a, r, s' \rangle, \langle \bar{s}, \bar{a}, \bar{s}' \rangle) \\ &= -\log P_\theta^G(s' | \bar{s}') - \log P_\theta^R(r | \bar{s}, \bar{a}) - \log \bar{\pi}_\theta(\bar{a} | \bar{s}) + \log \phi_\iota(\bar{s}' | s') \\ & \quad - \mathbf{1}_{(\bar{\mathcal{A}}, \mathcal{A})} \cdot \log \bar{\mathbf{P}}_{\bar{\pi}_\theta}(\bar{s}' | \bar{s}) - \mathbf{1}_{\neq}(\bar{\mathcal{A}}, \mathcal{A}) \cdot (\log \psi_\theta(a | \bar{s}, \bar{a}) + \log \bar{\mathbf{P}}_\theta(\bar{s}' | \bar{s}, \bar{a}) - \log Q_\iota^A(\bar{a} | \bar{s}, a)). \end{aligned}$$

Notice that we cannot assign directly $p_{\langle s, a, r, s' \rangle}$ to L_{ELBO} since priorities require to be strictly positive to compute the replay buffer distribution. A solution is to pass $L_{\text{ELBO}}(\langle s, a, r, s' \rangle, \langle \bar{s}, \bar{a}, \bar{s}' \rangle)$ to the logistic function, i.e.,

$$p_{\langle s, a, r, s' \rangle} = x^* \cdot \sigma(k \cdot (L_{\text{ELBO}}(\langle s, a, r, s' \rangle, \langle \bar{s}, \bar{a}, \bar{s}' \rangle) - x_0))$$

where $x^* > 0$ is the scale, $k > 0$ is the growth rate, and x_0 is the location of the logistic. In practice, we set x^* to the desired maximum priority and we maintain upper (L^{max}) and lower bounds (L^{min}) on the loss during learning. Along training steps, we tune these values according to the current loss and we set $x_0 = \frac{L^{\text{max}} - L^{\text{min}}}{2}$ and $k = \frac{x^*}{L^{\text{max}} - L^{\text{min}}}$.

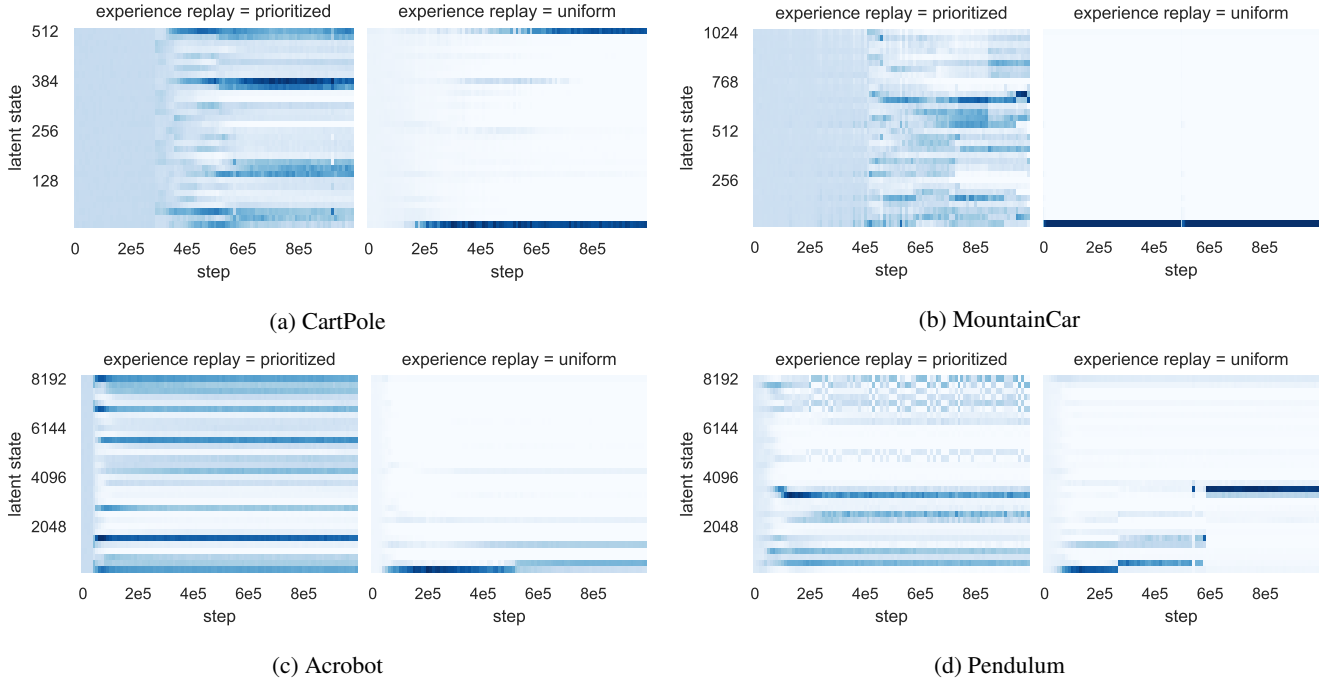


Figure 3: Latent space distribution along training steps. The intensity of the blue hue corresponds to the frequency of latent states produced by ϕ during training. We compare a bucket-based prioritized against a simple uniform experience replay. The latent space learned with transitions sampled from the uniform replay buffer collapses to (a) two, (b) a single, (c) and (d) few latent state(s).

D Details on RL Policy Distillation

Concretely, the goal of $\bar{\pi}_\theta$ is to mimic the behavior of π through the latent spaces. However, executing $\bar{\pi}_\theta$ in \mathcal{M} via ϕ_i and $\psi_{i,\theta}$ as described in Sect. 3 to evaluate our latent space model (e.g., Lem. 3.4) may result in performance loss compared to that offered under π . This is due to the abstraction learned via the ELBO: we do not expect a zero-distortion by encoding the state-action space through the VAE (and $\mathcal{M}_{\bar{\pi}_\theta}$ to behave exactly like \mathcal{M}_π), but to minimize it. Due to this remaining distortion, decisions taken according to $\bar{\pi}_\theta$ may result in unreachable states under π , causing $\bar{\pi}_\theta$ to behave poorly in that particular states since the learning process only allows to learn from transitions produced via π . We propose two approaches that can be used alone or together to alleviate this problem.

Globally-robust RL policy. In general, policies π learned through deep-RL provide *local* performance, meaning they provide good performance in states $s \in \mathcal{S}$ that are likely to be reached from s_I by executing π . It is, however, often suitable to distill and verify *globally-robust* RL policies, i.e., policies trained to provide good *global* performance, in a wider range of states, in particular those that are likely to be reached through the distillation. Training globally robust RL policies can be achieved by allowing the agent to learn (or pursuing its training) in a modified version of \mathcal{M} , where s_I is picked at random from \mathcal{S} . Training π this way will usually take longer since this may require more exploration. The degree of randomness can be decided according to the exploration/exploitation trade-off and the additional training time allowed. Moreover, we argue that this additional time is acceptable in our context since enabling and applying model checking are time-consuming tasks by nature.

ε -mimic. Assuming π is sufficiently robust for the distillation, we allow the encoder to process states reachable under both $\bar{\pi}_\theta$ and π by learning from a mixture $\hat{\pi}_\theta^\varepsilon$ of the two, defined as $\hat{\pi}_\theta^\varepsilon(a | s) = \pi(a | s) \cdot (1 - \varepsilon) + \bar{\pi}_\theta(a | s) \cdot \varepsilon$ for all $s \in \mathcal{S}$, $a \in \mathcal{A}$, given $\varepsilon \in [0, 1]$. Given the robustness assumption, states entered according to a decision $a \sim \bar{\pi}_\theta(\cdot | s)$ (produced with probability ε) should be efficiently processed by π . In practice, we start with a high value of ε (e.g., $\varepsilon = 1/2$) to encourage exploration of states possibly reachable under $\bar{\pi}_\theta$ and we anneal it to 0 during training.

E Experiments

E.1 Setup

We used TENSORFLOW 2.4.1 (Abadi et al. 2015) to implement the neural networks modeling our parameterized distributions constituting our variational model, optimize the loss function (ELBO), and running our PAC approximation schemes. Precisely, we used TENSORFLOW PROBABILITY 0.12.2 (Dillon et al. 2017) to handle the probabilistic components of the VAE (e.g.,

	CartPole	MountainCar	Acrobot	Pendulum	LunarLander
activation	leaky relu	leaky relu	relu	relu	relu
learning rate	10^{-3}	10^{-3}	10^{-4}	10^{-4}	10^{-4}
RL policy	DQN	DQN	DQN (robust)	SAC (robust)	SAC
$\log_2 \mathcal{S} $	9	10	13	13	16
$ \mathcal{A} $	/	/	/	3	5
$\lambda_{\bar{S}}^{\bar{S}}$	2/3	2/3	2/3	2/3	2/3
$\lambda_{\bar{A}}^{\bar{A}}$	1/2	1/2	1/2	1/2	1/2
$\lambda_{\bar{S}}^{\bar{A}}$	/	/	/	1/2	1/4
$\lambda_{\bar{A}}^{\bar{A}}$	/	/	/	1/3	1/6
τ_{λ_1}	10^{-6}	10^{-6}	10^{-6}	10^{-6}	10^{-6}
τ_{λ_2}	$2 \cdot 10^{-6}$	$2 \cdot 10^{-6}$	$2 \cdot 10^{-6}$	$2 \cdot 10^{-6}$	$2 \cdot 10^{-6}$
α	10^1	10^1	10^1	10^1	10^1
α_A	/	/	/	1	10^{-1}
τ_α	10^{-5}	10^{-5}	$7.5 \cdot 10^{-5}$	$7.5 \cdot 10^{-5}$	10^{-5}
τ_β	$5 \cdot 10^{-5}$	$5 \cdot 10^{-5}$	$7.5 \cdot 10^{-5}$	$7.5 \cdot 10^{-5}$	$5 \cdot 10^{-5}$
prioritized experience replay	bucket	bucket	bucket	loss	loss
ς	1/3	1/3	$3 \cdot 10^{-1}$	$3 \cdot 10^{-1}$	$3 \cdot 10^{-1}$
τ_ω	$7 \cdot 10^{-5}$	$7.5 \cdot 10^{-5}$	$7 \cdot 10^{-5}$	10^{-5}	10^{-5}
ε	0	0	1/2	1/2	0
τ_ε	/	/	10^{-5}	10^{-5}	/

Table 1: Hyper-parameter choices for the different environments. We write λ_Y^X for the temperature parameter used for the concrete relaxation of Bernoulli distributions when $X = \bar{S}$ (resp. Categorical distributions when $X = \bar{A}$). This is the encoder distribution if $Y = 1$ and the one of the latent transition function (resp. distilled policy) else, if $Y = 2$. Moreover, we write α_A for the scale factor of the action entropy regularizer where the final entropy regularization term is $\alpha \cdot (H(Q_L) + \alpha_A \cdot H(Q_L^A))$.

distributions, reparameterization tricks, etc.), as well as TF-AGENTS 0.7.1 (Guadarrama et al. 2018) to handle the RL parts of the framework, coupled with REVERB replay buffers (Cassirer et al. 2021).

The experiments have been driven on a cluster running under CentOS Linux 7 (Core) composed of a mix of nodes containing Intel processors with the following CPU microarchitectures: (i) 10-core INTEL E5-2680v2, (ii) 14-core INTEL E5-2680v4, and (iii) 20-core INTEL Xeon Gold 6148. We used 8 cores and 128 GB of memory for each of our experiments.

E.2 Hyper-parameters

Each distribution parameters (locations, scales, logits) are inferred by neural networks (multilayer perceptrons) composed of two dense hidden layers and 256 cells by layer. For all our experiments, we used the TENSORFLOW’s implementation of the Adam optimizer (Kingma and Ba 2015) to learn the neural networks weights. We fixed the size of the prioritized experience replay to 10^6 . The training starts when the agent has collected 10^4 transitions in \mathcal{M} . Every time a transition is added to the replay buffer, its priority is set to the maximum value. We used minibatches of size 128 to optimize the loss function (i.e., ELBO) and we applied a minibatch update every time the agent executing π performed 16 steps in \mathcal{M} . This allows the VAE to process at least $1/8$ of the new transitions collected by sampling from the replay buffer (more details in Schaul et al. 2016). We fixed ω to 0.4 as suggested by Schaul et al. (2016).

Annealing schemes. During training, we anneal different hyper-parameters to 0 or 1 according to the following annealing schemes: (i) we start annealing the parameters at step $t_0 = 10^4$, (ii) let $\zeta \in [0, \infty]$, we anneal ζ to 0 via $\zeta_t = \zeta \cdot (1 - \tau_\zeta)^{t-t_0}$, or (iii) let $\zeta \in [0, 1]$, we anneal ζ to 1 via $\zeta_t = \zeta + (1 - \zeta) \cdot (1 - (1 - \tau_\zeta)^{t-t_0})$ for step $t > t_0$ and annealing term τ_ζ .

Unshared parameters. The list of single hyper-parameters used for the different environments is given in Table 1. The activation function of all cells of the neural networks was chosen between relu and leaky relu, the learning rate of the optimizer in $[10^{-4}, 10^{-3}]$, the regularizer scale factor α from $\{0.1, 1, 10, 100\}$, ς in $[0, 1]$, the values of each annealing term in $[10^{-6}, 10^{-4}]$, and we tested both loss- and bucket-based experience replay buffers.

E.3 Discrete Latent Dynamics

As pointed out by Corneil, Gerstner, and Brea (2018), the latent transition function learned via the continuous relaxation takes a simple form when discretized (i.e., when $\lambda_{P_\theta} \rightarrow 0$): the latent variables produced this way via \bar{P}_θ are independent Bernoullis, meaning each bit of $\bar{s}' \sim \bar{P}_\theta(\cdot | \bar{s}, \bar{a})$ are independent, for any $\bar{s} \in \bar{S}$, $\bar{a} \in \bar{A}$. To remedy this, we adopt the approach of Corneil,

Environment	$\mathcal{S} \subseteq$	Description, for $\mathbf{s} \in \mathcal{S}$	Labeling function $\ell(\mathbf{s})$	$\mathbf{AP} = \{p_1, \dots, p_n\}$
CartPole	\mathbb{R}^4	<ul style="list-style-type: none"> \mathbf{s}_1: cart position \mathbf{s}_2: cart velocity \mathbf{s}_3: pole angle (rad) \mathbf{s}_4: pole velocity at tip 	$\langle \mathbf{1}_{<}(\mathbf{s}_1, 1.5),$ $\mathbf{1}_{<}(\mathbf{s}_3, 0.15) \rangle$	<ul style="list-style-type: none"> p_1: safe cart position p_2: safe pole angle
MountainCar	\mathbb{R}^2	<ul style="list-style-type: none"> \mathbf{s}_1: position \mathbf{s}_2: velocity 	$\langle \mathbf{1}_{\geq}(\mathbf{s}_1, 1/2),$ $\mathbf{1}_{\geq}(\mathbf{s}_1, -1/2),$ $\mathbf{1}_{\geq}(\mathbf{s}_2, 0) \rangle$	<ul style="list-style-type: none"> p_1: target position p_2: right-hand side of the mountain p_3: car going forward
Acrobot	\mathbb{R}^6	Let $\theta_1, \theta_2 \in [0, 2\pi]$ be the angles of the two rotational joints, <ul style="list-style-type: none"> $\mathbf{s}_1 = \cos(\theta_1)$ $\mathbf{s}_2 = \sin(\theta_1)$ $\mathbf{s}_3 = \cos(\theta_2)$ $\mathbf{s}_4 = \sin(\theta_2)$ \mathbf{s}_5: angular velocity 1 \mathbf{s}_6: angular velocity 2 	$\langle \mathbf{1}_{>}(-\mathbf{s}_1 - \mathbf{s}_3 \cdot \mathbf{s}_1 + \mathbf{s}_4 \cdot \mathbf{s}_2, 1),$ $\mathbf{1}_{\geq}(\mathbf{s}_1, 0),$ $\mathbf{1}_{\geq}(\mathbf{s}_2, 0)$ $\mathbf{1}_{\geq}(\mathbf{s}_3, 0)$ $\mathbf{1}_{\geq}(\mathbf{s}_4, 0)$ $\mathbf{1}_{\geq}(\mathbf{s}_5, 0)$ $\mathbf{1}_{\geq}(\mathbf{s}_6, 0) \rangle$	<ul style="list-style-type: none"> p_1: RL agent target p_2: $\theta_1 \in [0, \pi/2] \cup [3\pi/2, 2\pi]$ p_3: $\theta_1 \in [0, \pi]$ p_4: $\theta_2 \in [0, \pi/2] \cup [3\pi/2, 2\pi]$ p_5: $\theta_2 \in [0, \pi]$ p_6: positive angular velocity (1) p_7: positive angular velocity (2)
Pendulum	\mathbb{R}^3	Let $\theta \in [0, 2\pi]$ be the joint angle <ul style="list-style-type: none"> $\mathbf{s}_1 = \cos(\theta)$ $\mathbf{s}_2 = \sin(\theta)$ \mathbf{s}_3: angular velocity 	$\langle \mathbf{1}_{\geq}(\mathbf{s}_1, \cos(\pi/3)),$ $\mathbf{1}_{\geq}(\mathbf{s}_1, 0),$ $\mathbf{1}_{\geq}(\mathbf{s}_2, 0)$ $\mathbf{1}_{\geq}(\mathbf{s}_3, 0) \rangle$	<ul style="list-style-type: none"> p_1: safe joint angle p_2: $\theta \in [0, \pi/2] \cup [3\pi/2, 2\pi]$ p_3: $\theta \in [0, \pi]$ p_4: positive angular velocity
LunarLander	\mathbb{R}^8	<ul style="list-style-type: none"> \mathbf{s}_1: horizontal coordinates \mathbf{s}_2: vertical coordinates \mathbf{s}_3: horizontal speed \mathbf{s}_4: vertical speed \mathbf{s}_5: ship angle \mathbf{s}_6: angular speed \mathbf{s}_7: left leg contact \mathbf{s}_8: right leg contact 	based on the heuristic function	<ul style="list-style-type: none"> p_1: unsafe angle p_2: leg ground contact p_3: lands too rapidly p_4: left inclination p_5: right inclination p_6: motors shut down

Table 2: Labeling functions used in our experiments. We provide a short description of the state space and the meaning of the atomic propositions forming the labels. Recall that labels and \mathbf{AP} are respectively binary and one-hot encoded. Let $n = |\mathbf{AP}|$ with $\mathbf{AP} = \{p_1, \dots, p_n\}$, we write p_i for the one-hot vector of size n with the i^{th} entry set to 1, with $i \in [n] \setminus \{0\}$. The LunarLander labeling function is based on the heuristic function of the OpenAI’s implementation (Brockman et al. 2016).

Gerstner, and Brea (2018) and we reconstruct the latent dynamics via *frequency estimation* (e.g., Bazille et al. 2020) to check the abstraction quality in a PAC manner (cf. Fig. 2): for each environment, we evaluated the latent space model quality based on frequency-estimated latent dynamics from transitions collected by (repeatedly) simulating the environment for $2 \cdot 10^5$ steps.

E.4 Labeling functions

The labeling functions ℓ we used for each environment are detailed in Table 2.

F Reproducibility of the Results

Seeding. The code we provide allows for setting random seeds to run the experiments, making the overall shape of the Figures we present in this paper reproducible. However, the exact values obtained in each particular instance are not: our prioritized experience replays (and those of TF-AGENTS) rely on REVERB replay buffers, handling randomness via the ABSEIL C++ library³ which does not allow for manual seeding. All other libraries using randomness are seeded properly.

Additional References

Abadi, M.; Agarwal, A.; Barham, P.; Brevdo, E.; Chen, Z.; Citro, C.; Corrado, G. S.; Davis, A.; Dean, J.; Devin, M.; Ghemawat, S.; Goodfellow, I.; Harp, A.; Irving, G.; Isard, M.; Jia, Y.; Jozefowicz, R.; Kaiser, L.; Kudlur, M.; Levenberg, J.; Mané, D.; Monga, R.; Moore, S.; Murray, D.; Olah, C.; Schuster, M.; Shlens, J.; Steiner, B.; Sutskever, I.; Talwar, K.; Tucker, P.; Vanhoucke, V.; Vasudevan, V.; Viégas, F.; Vinyals, O.; Warden, P.; Wattenberg, M.; Wicke, M.; Yu, Y.; and Zheng, X. 2015. TensorFlow: Large-Scale Machine Learning on Heterogeneous Systems. Software available from tensorflow.org.

Baier, C.; and Katoen, J. 2008. *Principles of model checking*. MIT Press. ISBN 978-0-262-02649-9.

³<https://abseil.io>

- Bazille, H.; Genest, B.; Jégourel, C.; and Sun, J. 2020. Global PAC Bounds for Learning Discrete Time Markov Chains. In Lahiri, S. K.; and Wang, C., eds., *Computer Aided Verification - 32nd International Conference, CAV 2020, Los Angeles, CA, USA, July 21-24, 2020, Proceedings, Part II*, volume 12225 of *Lecture Notes in Computer Science*, 304–326. Springer.
- Cassirer, A.; Barth-Maron, G.; Brevdo, E.; Ramos, S.; Boyd, T.; Sottiaux, T.; and Kroiss, M. 2021. Reverb: A Framework For Experience Replay.
- Dillon, J. V.; Langmore, I.; Tran, D.; Brevdo, E.; Vasudevan, S.; Moore, D.; Patton, B.; Alemi, A.; Hoffman, M.; and Saurous, R. A. 2017. TensorFlow Distributions. arXiv:1711.10604.
- Guadarrama, S.; Korattikara, A.; Ramirez, O.; Castro, P.; Holly, E.; Fishman, S.; Wang, K.; Gonina, E.; Wu, N.; Kokiopoulou, E.; Sbaiz, L.; Smith, J.; Bartók, G.; Berent, J.; Harris, C.; Vanhoucke, V.; and Brevdo, E. 2018. TF-Agents: A library for Reinforcement Learning in TensorFlow. <https://github.com/tensorflow/agents>. [Online; accessed 25-June-2019].
- Kingma, D. P.; and Ba, J. 2015. Adam: A Method for Stochastic Optimization. In Bengio, Y.; and LeCun, Y., eds., *3rd International Conference on Learning Representations, ICLR 2015, San Diego, CA, USA, May 7-9, 2015, Conference Track Proceedings*.